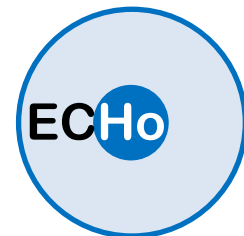




Kirchhoff-Institut für Physik

ECHo Experiment



Loredana Gastaldo
for the ECHo collaboration

Heidelberg University

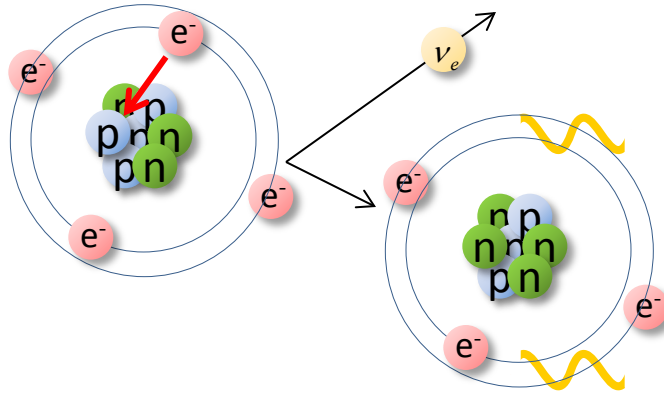


Contents

- Electron capture process: The case of ^{163}Ho
- Metallic Magnetic Calorimeters
- Recent results
- ECHo experiment

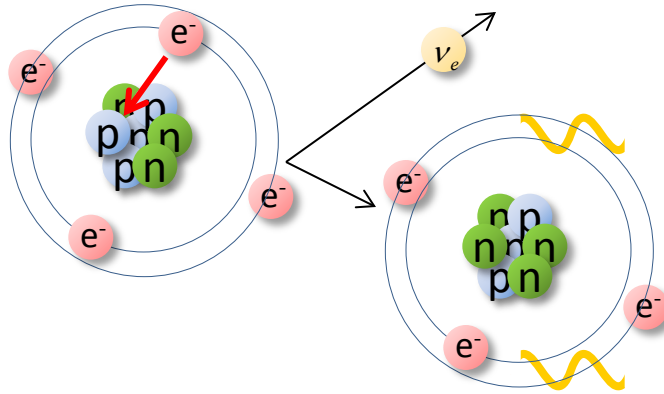


Electron Capture



A non-zero neutrino mass affects the **de-excitation energy spectrum**

Electron Capture

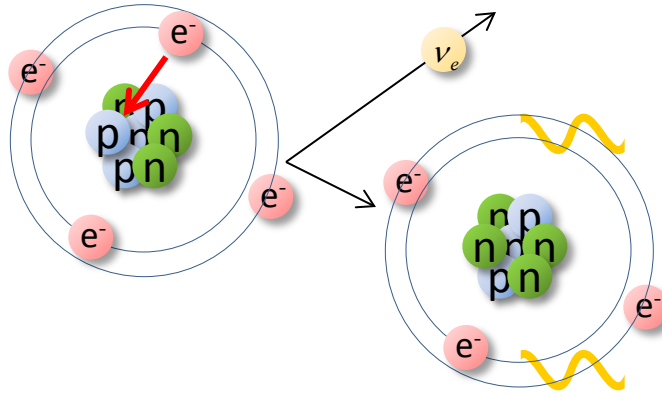


A non-zero neutrino mass affects the **de-excitation energy spectrum**

Atomic de-excitation:

- X-ray emission
- Auger electrons
- Coster-Kronig transitions

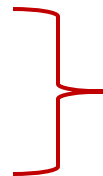
Electron Capture



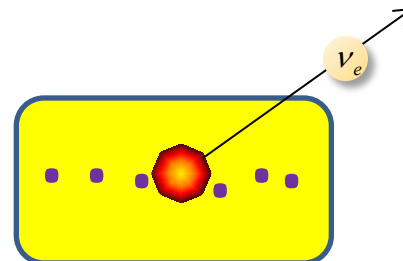
A non-zero neutrino mass affects the **de-excitation energy spectrum**

Atomic de-excitation:

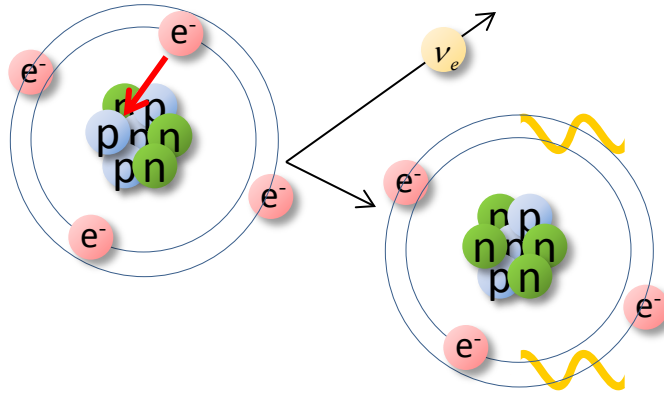
- X-ray emission
- Auger electrons
- Coster-Kronig transitions



Calorimetric measurement



Electron Capture



A non- zero neutrino mass affects the **de-excitation energy spectrum**

Atomic de-excitation:

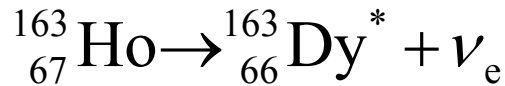
- X-ray emission
- Auger electrons
- Coster-Kronig transitions

}

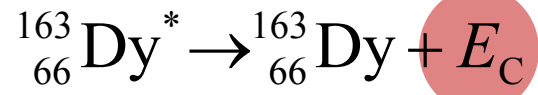
Calorimetric measurement

$$\frac{dW}{dE_C} = A(Q_{EC} - E_C)^2 \sqrt{1 - \frac{m_\nu^2}{(Q_{EC} - E_C)^2}} \sum_H B_H \varphi_H^2(0) \frac{\frac{\Gamma_H}{2\pi}}{(E_C - E_H)^2 + \frac{\Gamma_H^2}{4}}$$

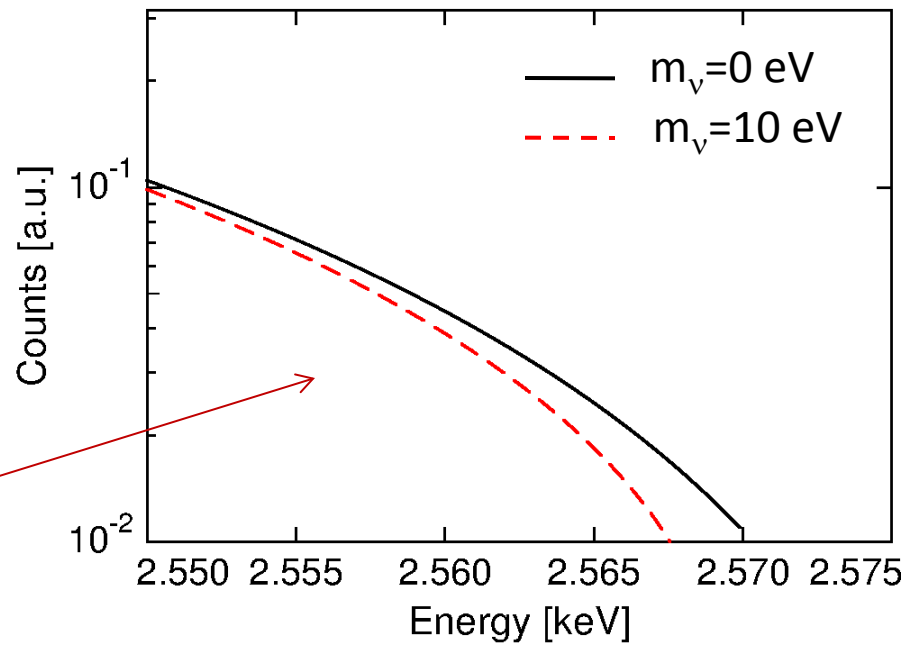
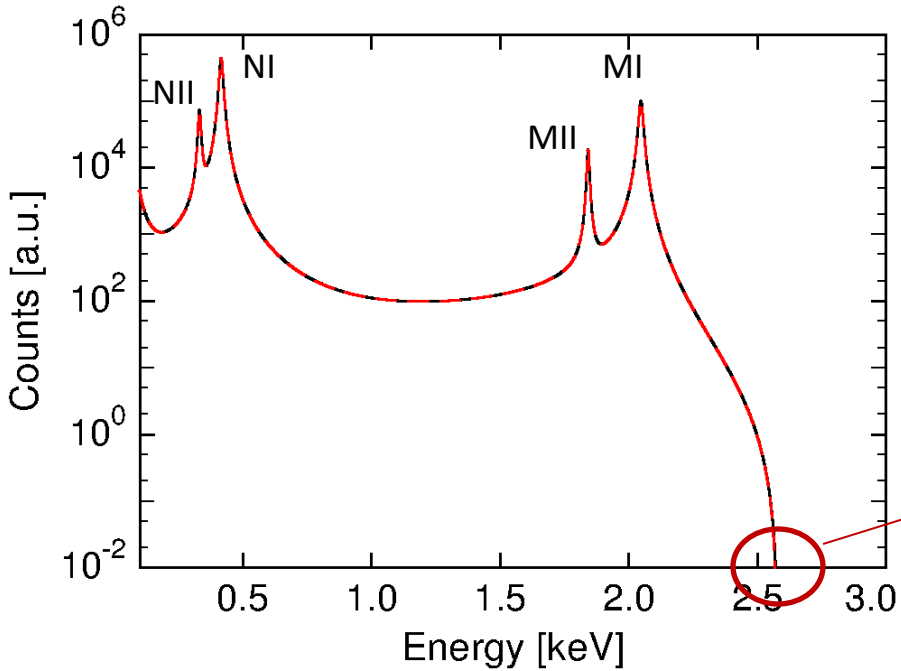
The case of ^{163}Ho



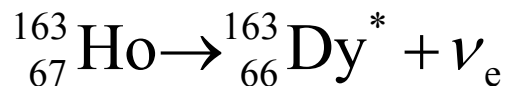
- $Q_{\text{EC}} \approx 2.5 \text{ keV}$



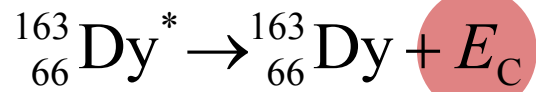
- $\tau_{1/2} \approx 4570 \text{ years}$



The case of ^{163}Ho



• $Q_{\text{EC}} \cong 2.5 \text{ keV}$



• $\tau_{1/2} \cong 4570 \text{ years}$

Volume 118B, number 4, 5, 6

PHYSICS LETTERS

9 December 1982

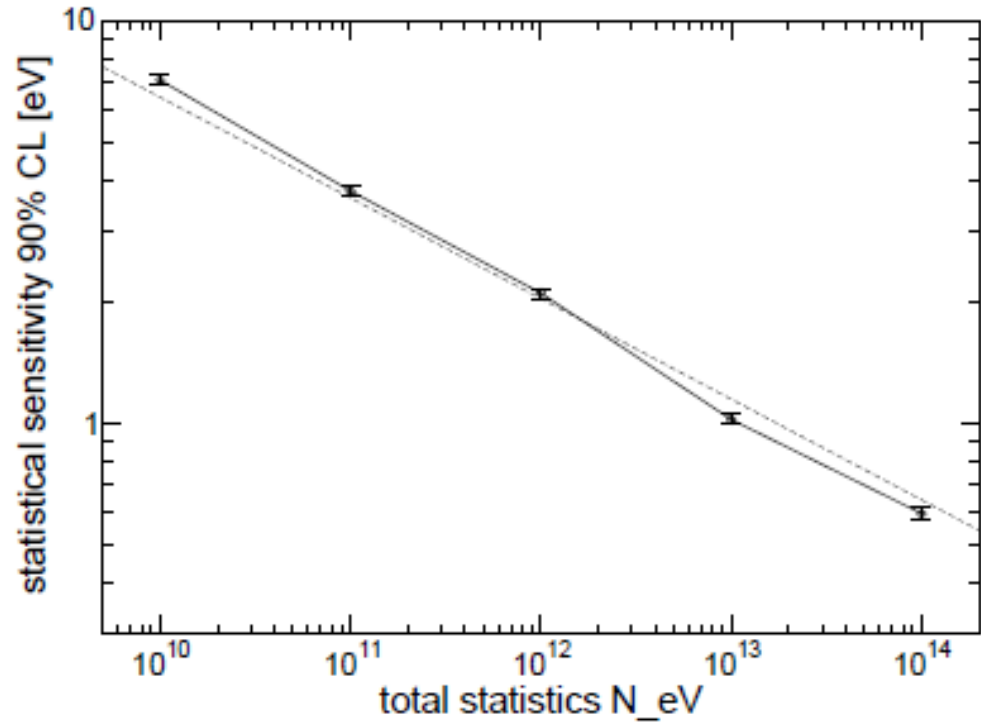
CALORIMETRIC MEASUREMENTS OF $^{163}\text{HOLMIUM}$ DECAY AS TOOLS TO DETERMINE THE ELECTRON NEUTRINO MASS

A. DE RÚJULA and M. LUSIGNOLI ¹

CERN, Geneva, Switzerland

The case of ^{163}Ho : Sub-eV sensitivity

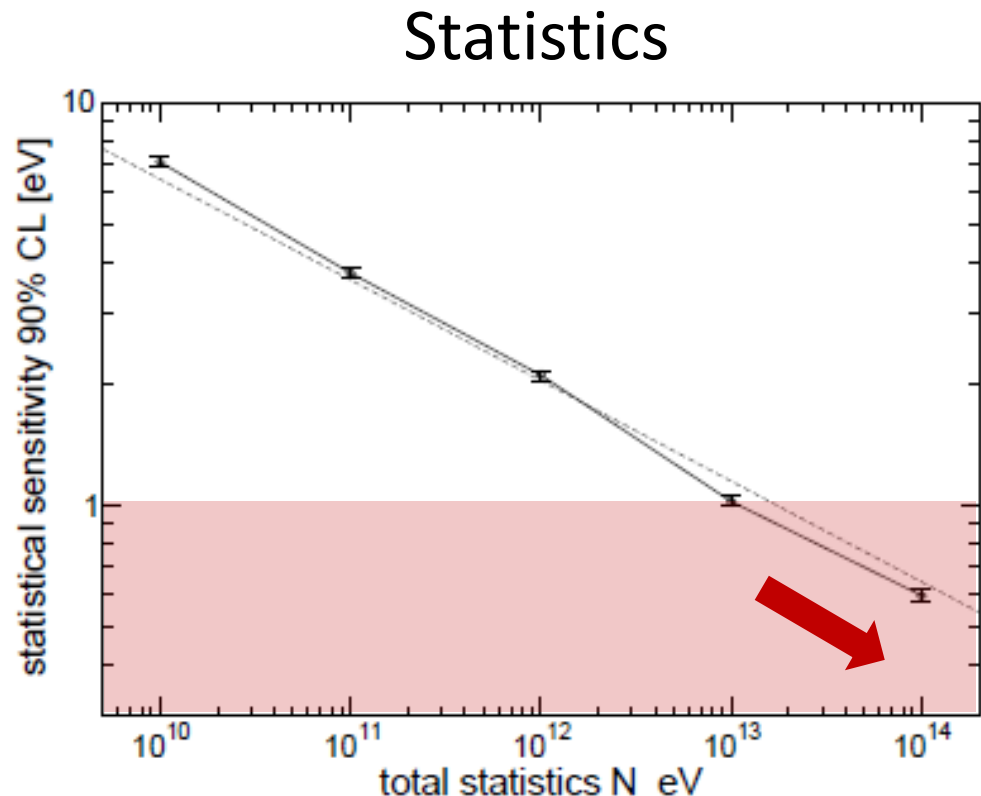
Statistics



$$\Delta E_{\text{FWHM}} = 1 \text{ eV}, f_{\text{pp}} = 10^{-5}, Q_{\text{EC}} = 2600 \text{ eV}$$

The case of ^{163}Ho : Sub-eV sensitivity

$N_{\text{ev}} > 10^{14}$

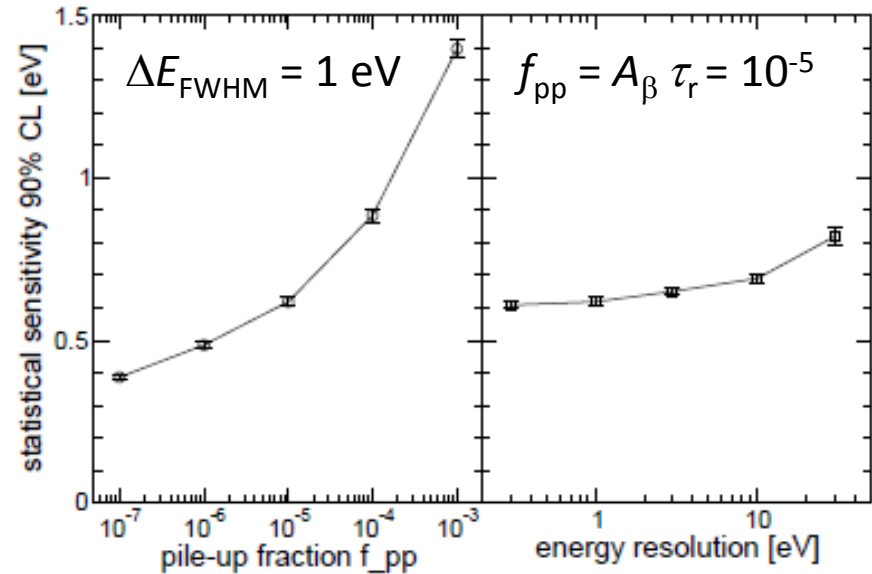


$$\Delta E_{\text{FWHM}} = 1 \text{ eV}, f_{\text{pp}} = 10^{-5}, Q_{\text{EC}} = 2600 \text{ eV}$$

The case of ^{163}Ho : Sub-eV sensitivity

$N_{\text{ev}} > 10^{14}$

Detector performance



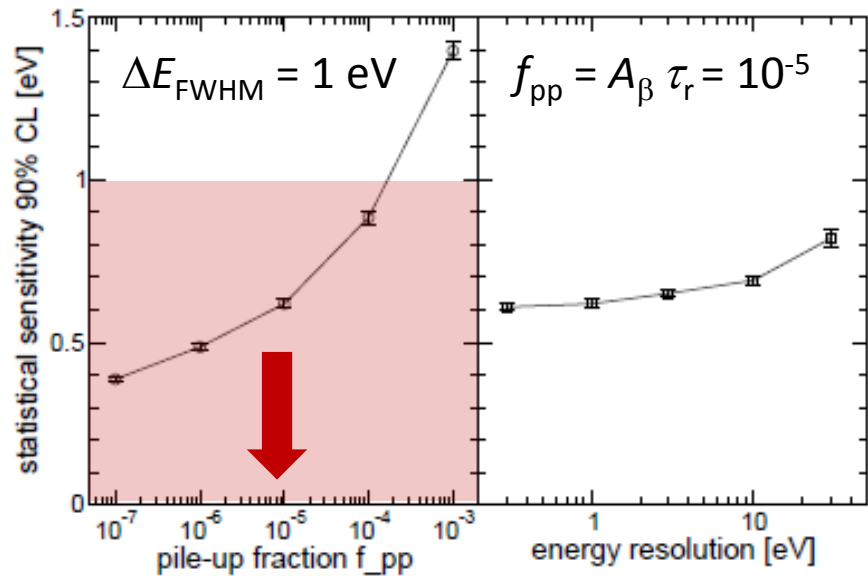
$$N_{\text{ev}} = 10^{14}, Q_{\text{EC}} = 2600 \text{ eV}$$

The case of ^{163}Ho : Sub-eV sensitivity

$$N_{\text{ev}} > 10^{14}$$

$$f_{\text{pp}} < 10^{-5}$$

Detector performance



$$N_{\text{ev}} = 10^{14}, Q_{\text{EC}} = 2600 \text{ eV}$$

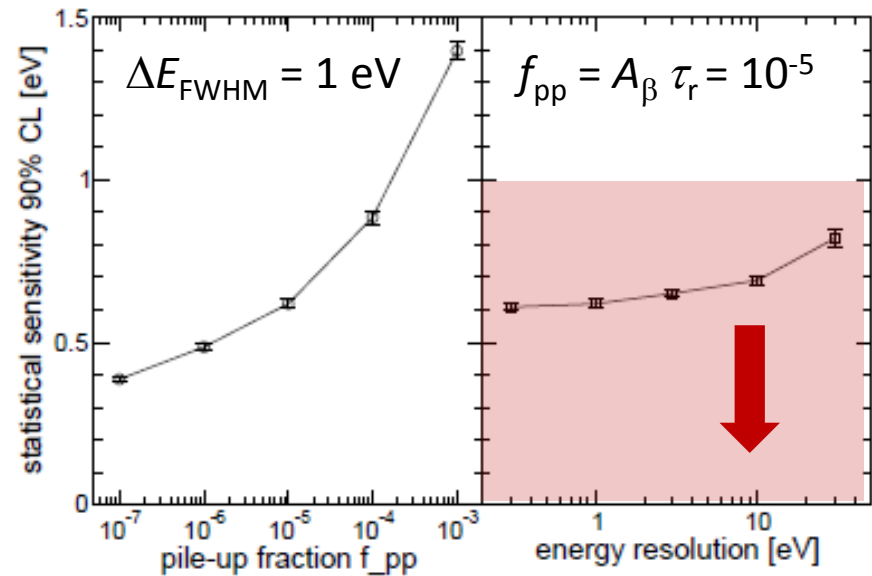
The case of ^{163}Ho : Sub-eV sensitivity

$$N_{\text{ev}} > 10^{14}$$

$$f_{\text{pp}} < 10^{-5}$$

$$\Delta E_{\text{FWHM}} < 10 \text{ eV}$$

Detector performance



$$N_{\text{ev}} = 10^{14}, Q_{\text{EC}} = 2600 \text{ eV}$$

The case of ^{163}Ho : Sub-eV sensitivity

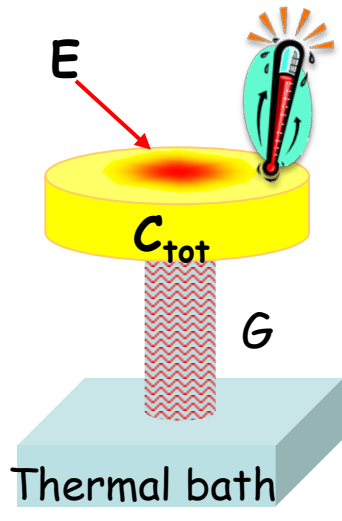
$$\begin{array}{ccc} N_{\text{ev}} > 10^{14} & \longrightarrow & \tau_r \sim 0.1 \mu\text{s} \\ f_{\text{pp}} < 10^{-5} & \longrightarrow & A_\beta \approx 10 \text{ s}^{-1} \\ \Delta E_{\text{FWHM}} < 10 \text{ eV} & & \end{array} \longrightarrow \geq 10^5 \text{ detectors}$$

The case of ^{163}Ho : Sub-eV sensitivity

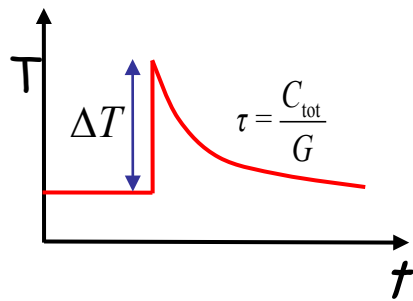
$$\begin{array}{ccc} N_{\text{ev}} > 10^{14} & \longrightarrow & \tau_r \sim 0.1 \mu\text{s} \\ f_{\text{pp}} < 10^{-5} & \longrightarrow & A_\beta \approx 10 \text{ s}^{-1} \\ \Delta E_{\text{FWHM}} < 10 \text{ eV} & & \end{array} \longrightarrow \geq 10^5 \text{ detectors}$$

Low temperature
Metallic Magnetic Calorimeter

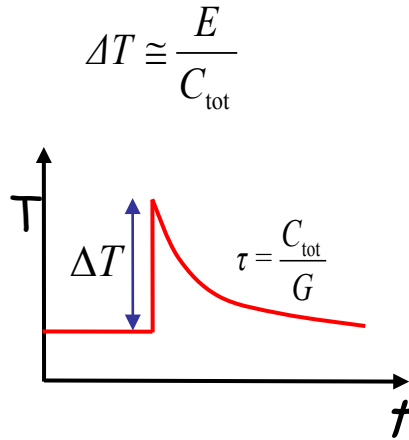
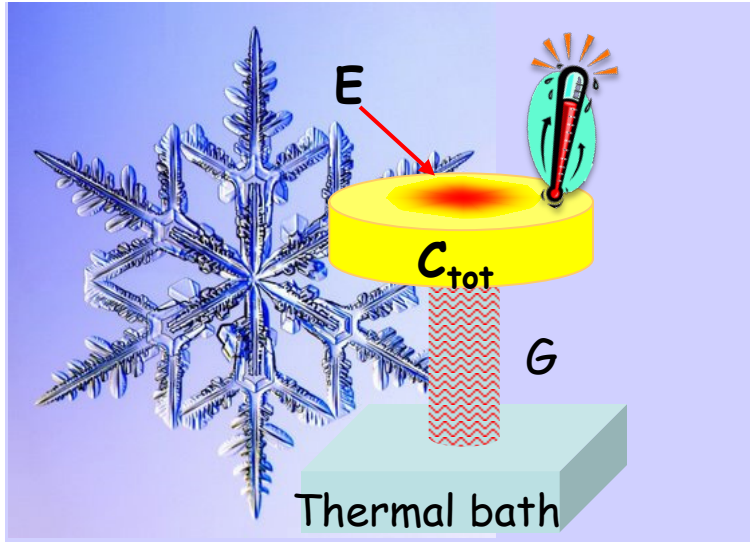
MMCs: Concept



$$\Delta T \approx \frac{E}{C_{\text{tot}}}$$

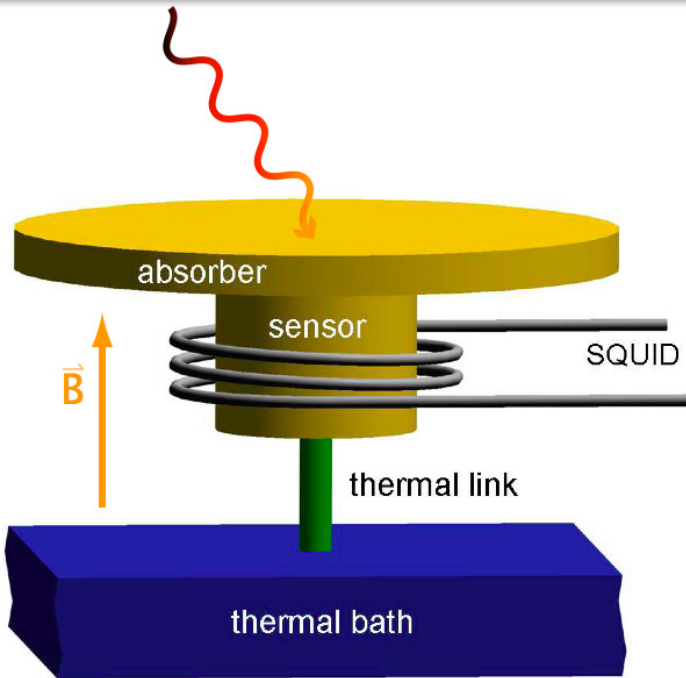


MMCs: Concept

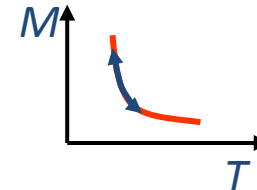


- Working temperature below 100 mK
 - small specific heat
 - large temperature change
 - small thermal noise
- Very sensitive temperature sensor

MMCs: Concept



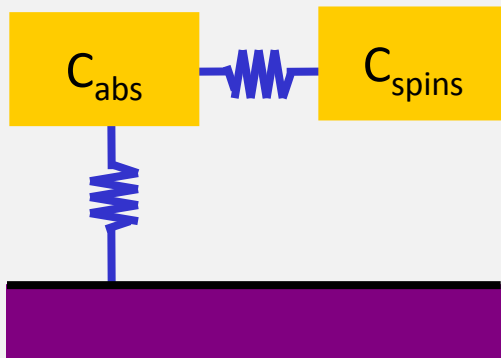
Paramagnetic sensor: Au:Er_{500ppm}



Signal size:

$$\delta M = \frac{\partial M}{\partial T} \delta T = \frac{\partial M}{\partial T} \frac{E_\gamma}{C_{\text{tot}}}$$

Energy resolution --- Why ,micro'-calorimeter

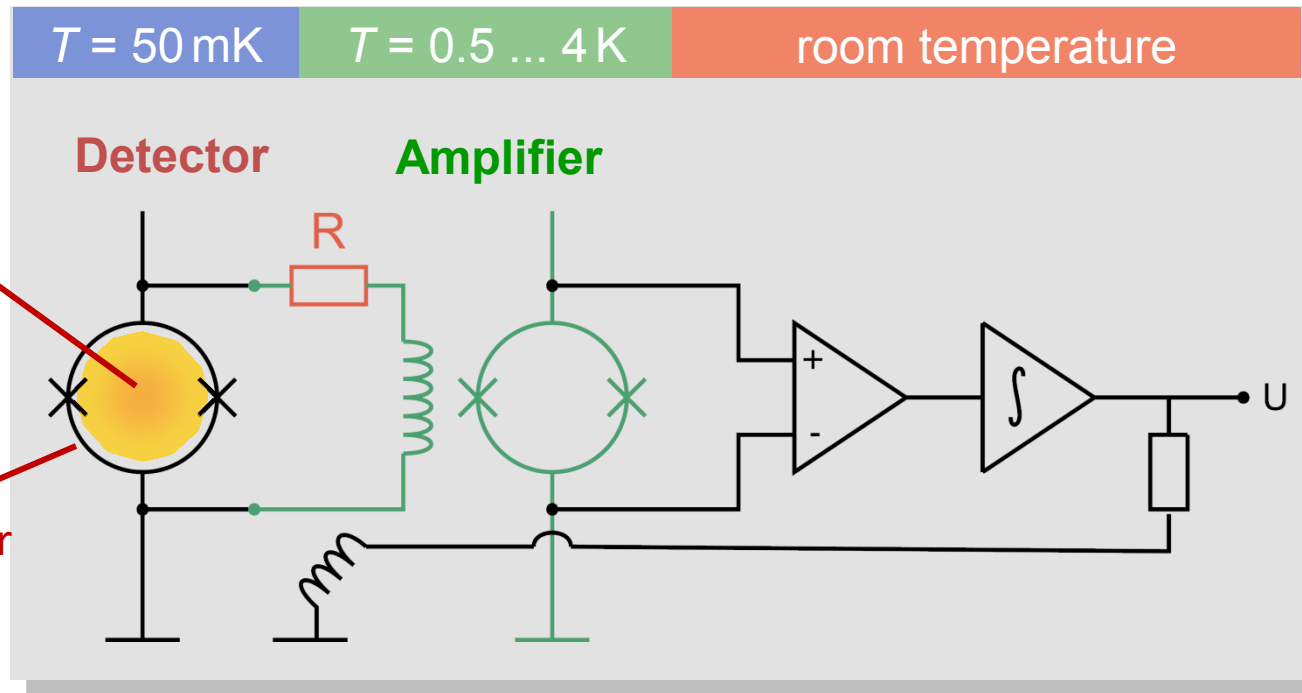


Thermal fluctuations of energy
between absorber, thermometer and bath lead to

$$\Delta E_{\text{FWHM}} \simeq 2,36 \sqrt{4k_B C_{\text{Abs}} T^2} \sqrt{2} \left(\frac{\tau_0}{\tau_1} \right)^{1/4}$$

e.g. **1eV** for $C = 1 \text{ pJ/K}$ at $T = 50 \text{ mK}$

MMCs: Readout



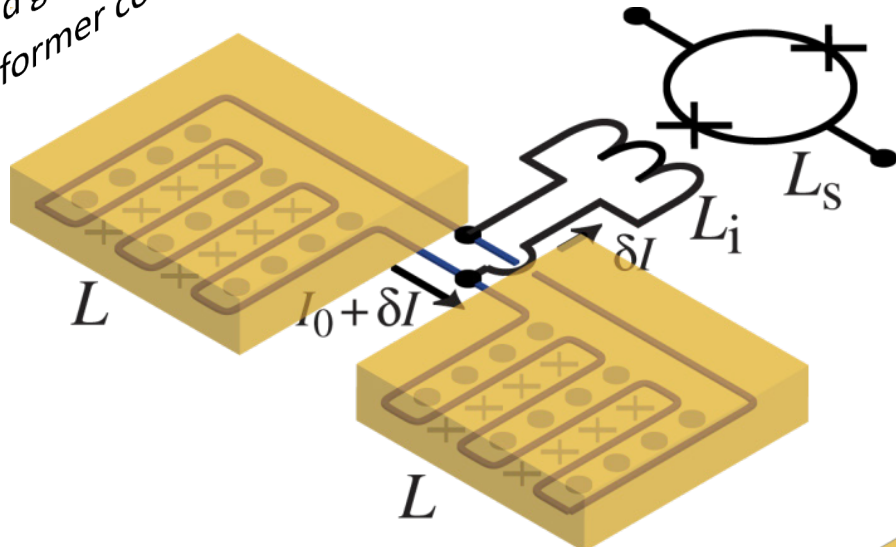
Two-stage SQUID setup with flux locked loop to linearize the first stage SQUID allows for:

- low noise
- large bandwidth / slewrate
- small power dissipation on detector SQUID chip (voltage bias)

MMCs: Geometries

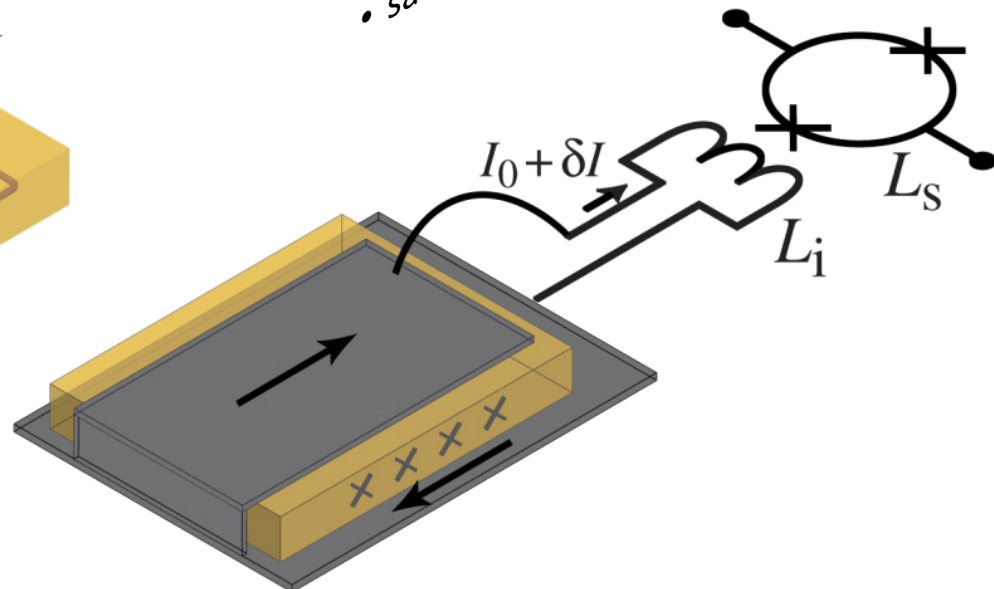
Well established:

- planar T-sensor
- superconducting meander shaped pickup loop
- B-field generated by persistent current
- transformer coupled to SQUID



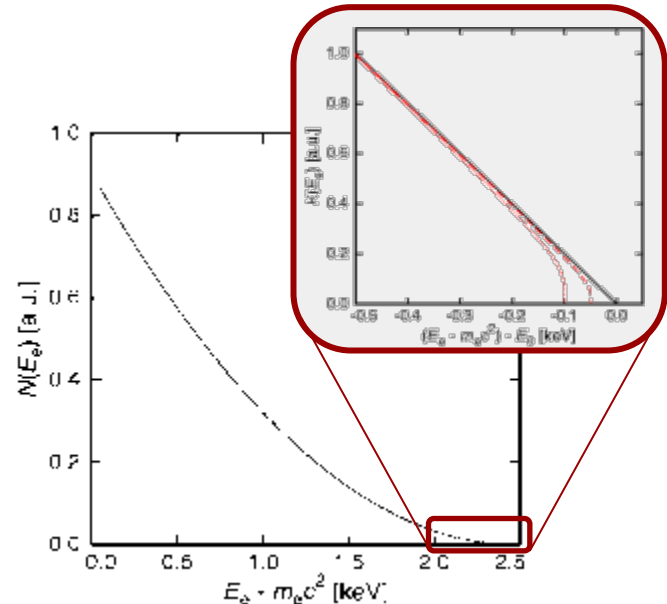
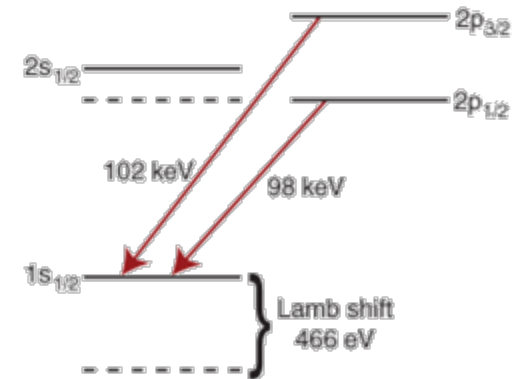
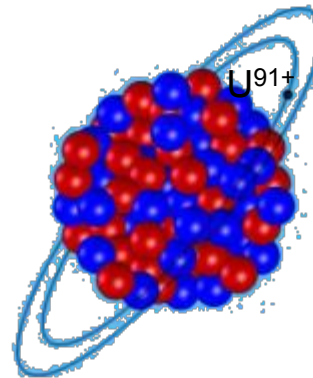
New sandwich geometry:

- best magn. flux coupling
- planar sensor
- sandwiched between stripline

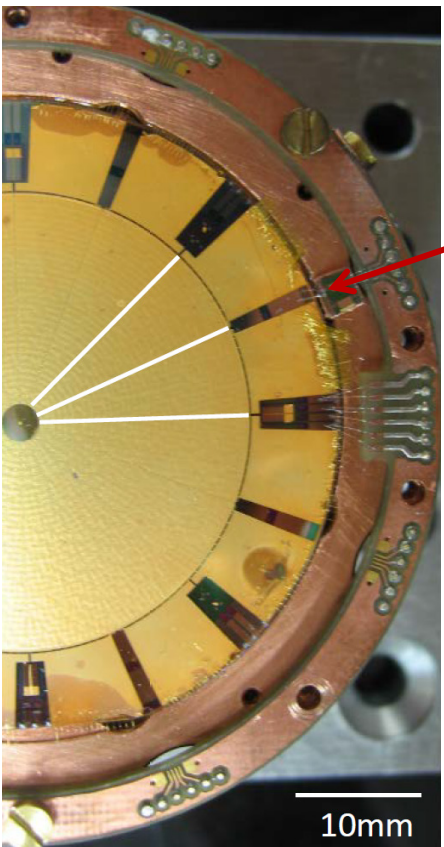


MMCs: Applications

- X-ray spectroscopy
 - atomic physics
 - astronomy
- X-ray imaging
 - large MMC arrays
 - microwave SQUID multiplexing
- Detection of molecular fragments
- Radiation standards for metrology
- Experiments for neutrino physics
 - β decay of ^{187}Re (MARE)
 - EC of ^{163}Ho (ECHO)
 - $0\nu2\beta$ (AMoRE & LUMINEU)



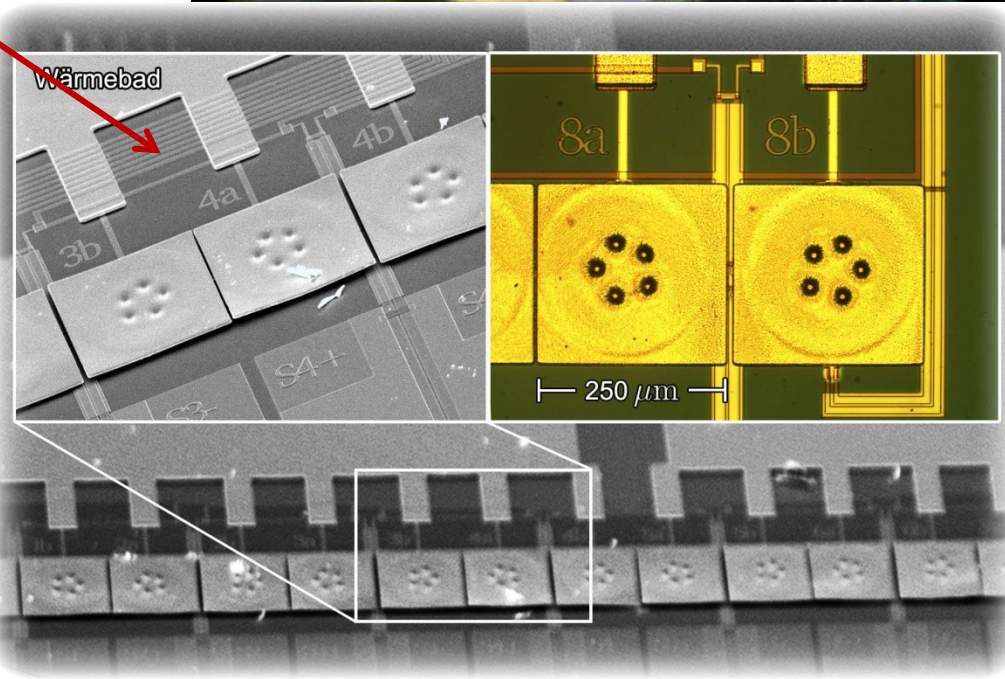
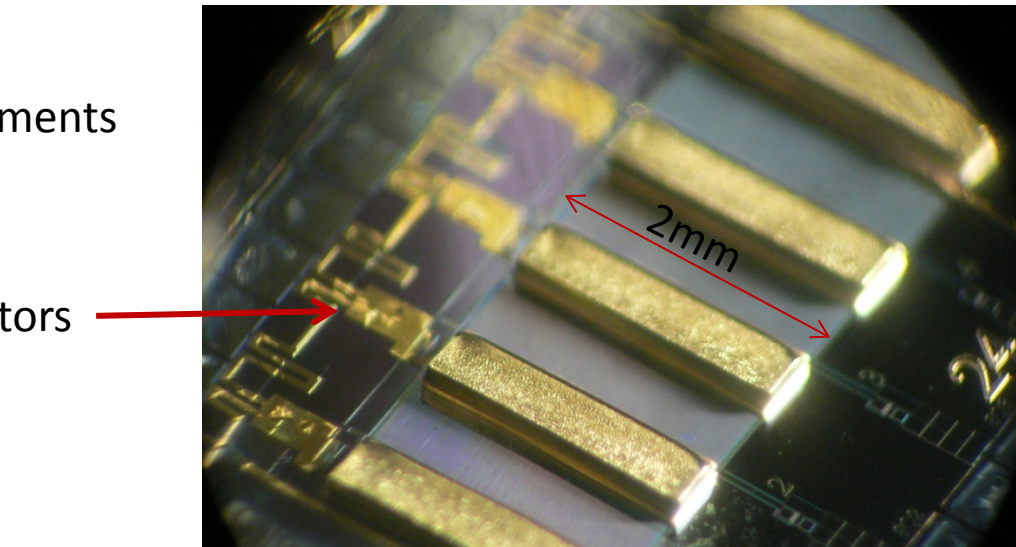
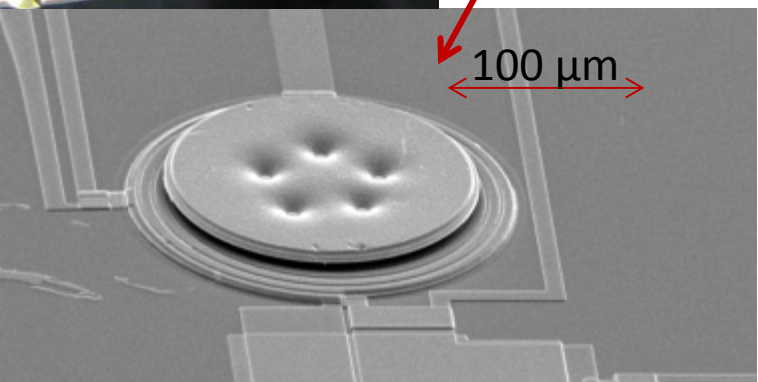
MMCs: Examples



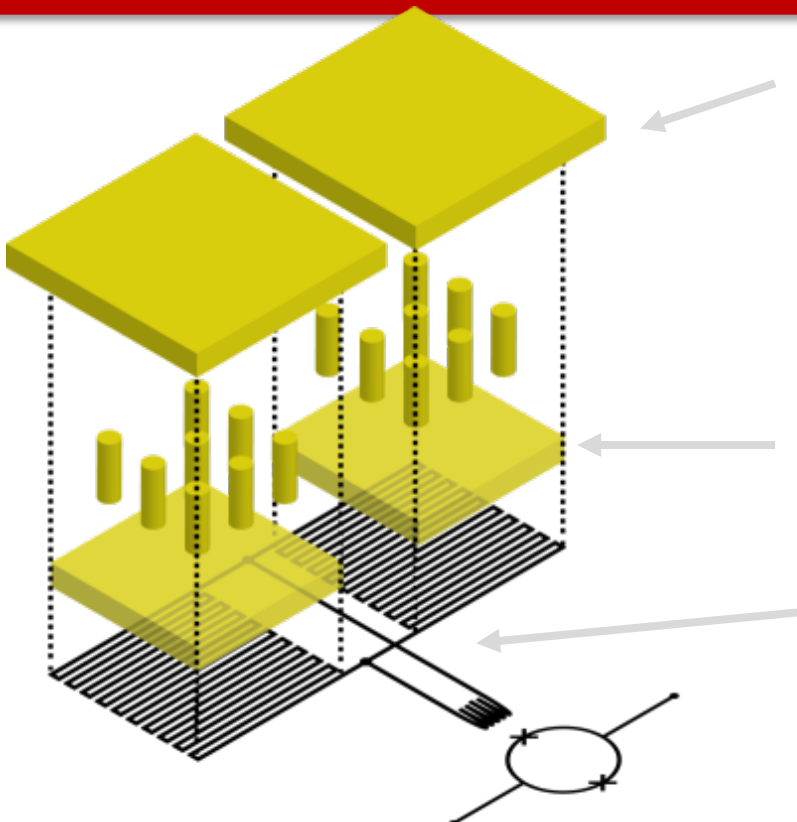
Pizza detector
for molecular fragments

Hard x-rays detectors

Soft x-rays
detectors



maXs: 1d-array for soft x-rays



- **1x8 x-ray absorbers**

- $250\mu\text{m} \times 250\mu\text{m}$ gold, $5\mu\text{m}$ thick
- $>98\%$ Qu.-Eff. @ 6 keV
- electroplated into photoresist mold ($\text{RRR}>15$)
- mech/therm contact to sensor by stems
to prevent loss of initial hot phonons

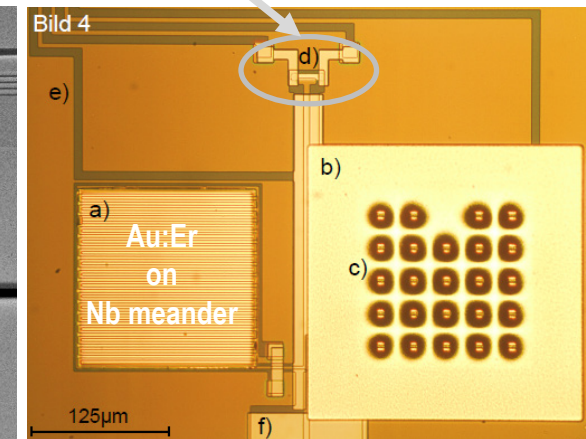
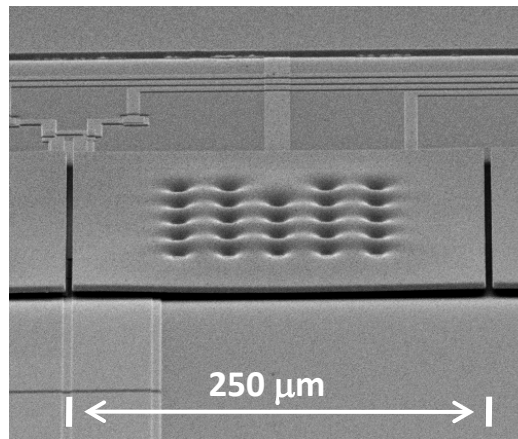
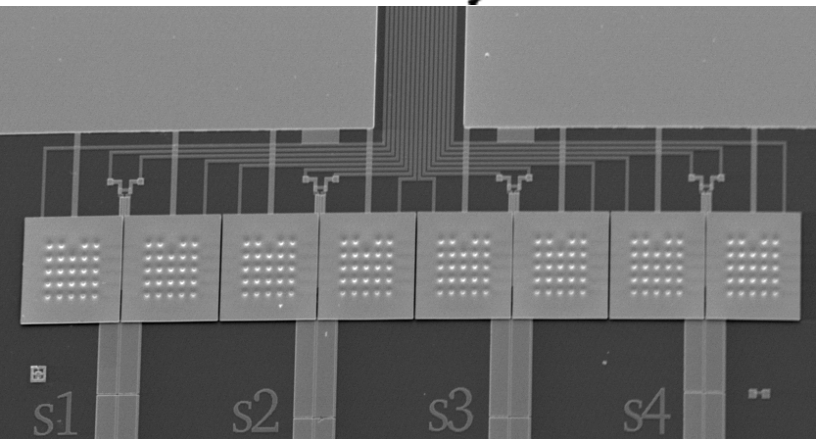
- **Au: $^{166}\text{Er}_{300\text{ppm}}$ temperature sensors**

- co-sputtered from pure Au and high conc. AuEr target

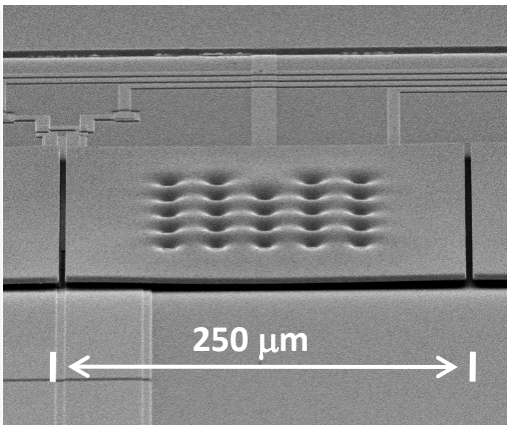
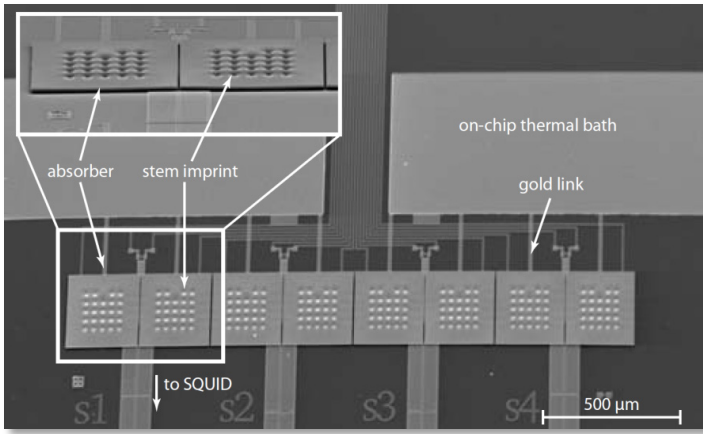
- **Meander shaped pickup coils**

- $2.5\ \mu\text{m}$ wide Nb lines, $\sim 400\ \text{nm}$ thick
- $I_c \approx 100\text{mA}$

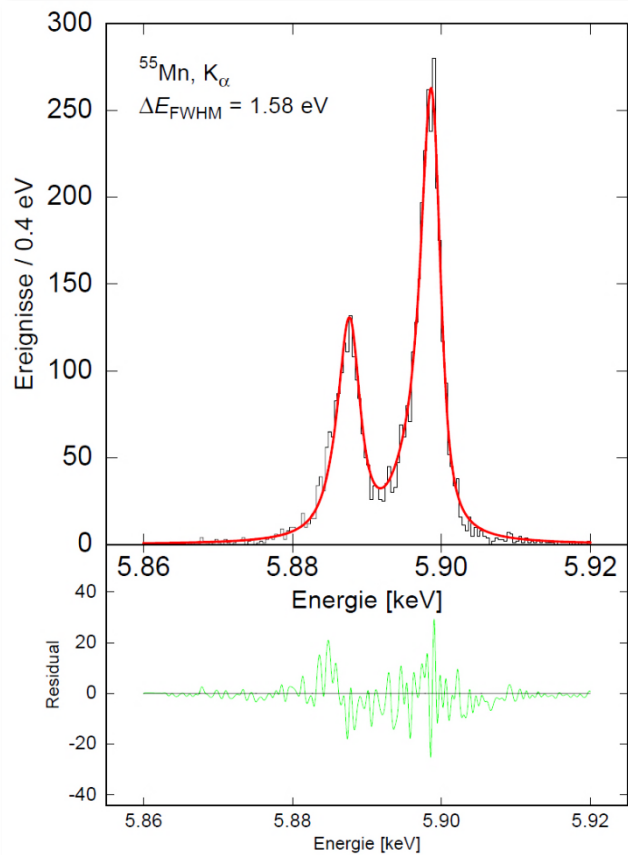
- **On-chip persistent current switch (AuPd)**



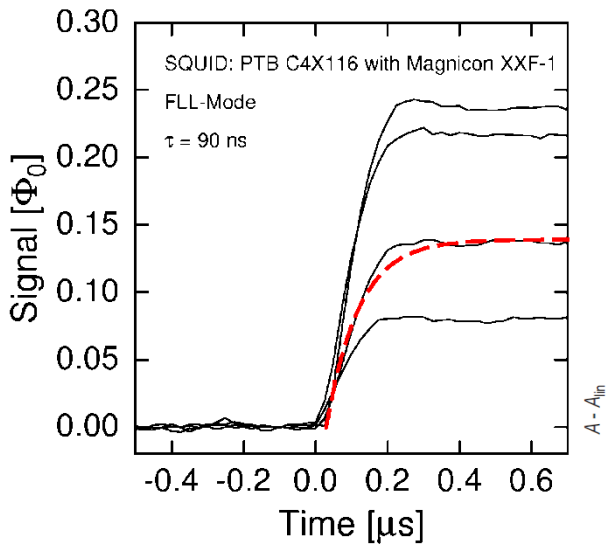
maXs: 1d-array for soft x-rays ($T=20$ mK)



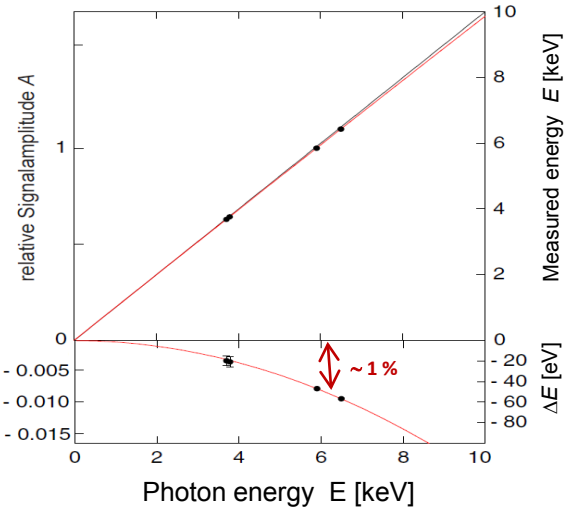
$$\Delta E_{FWHM} = 1.6 \text{ eV} @ 6 \text{ keV}$$



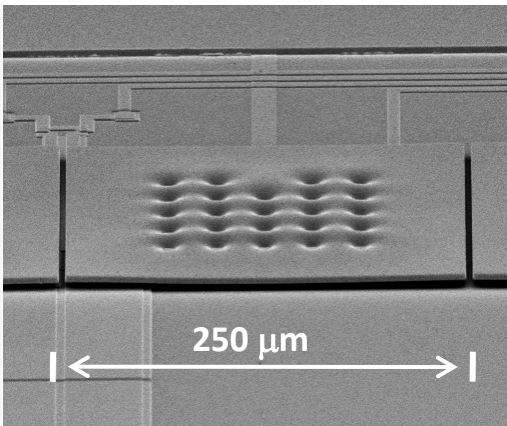
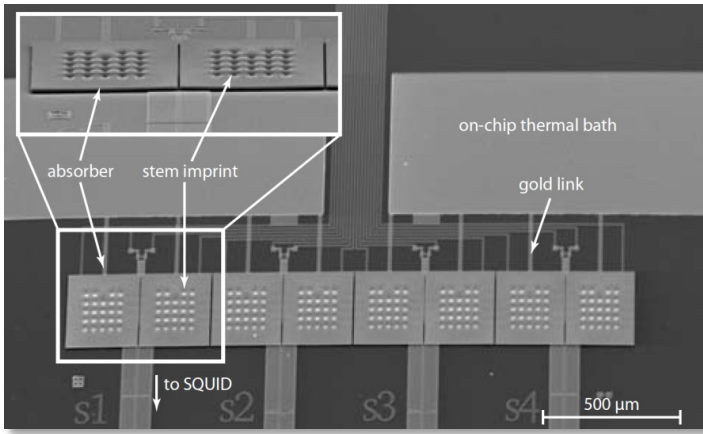
Rise Time: 90 ns



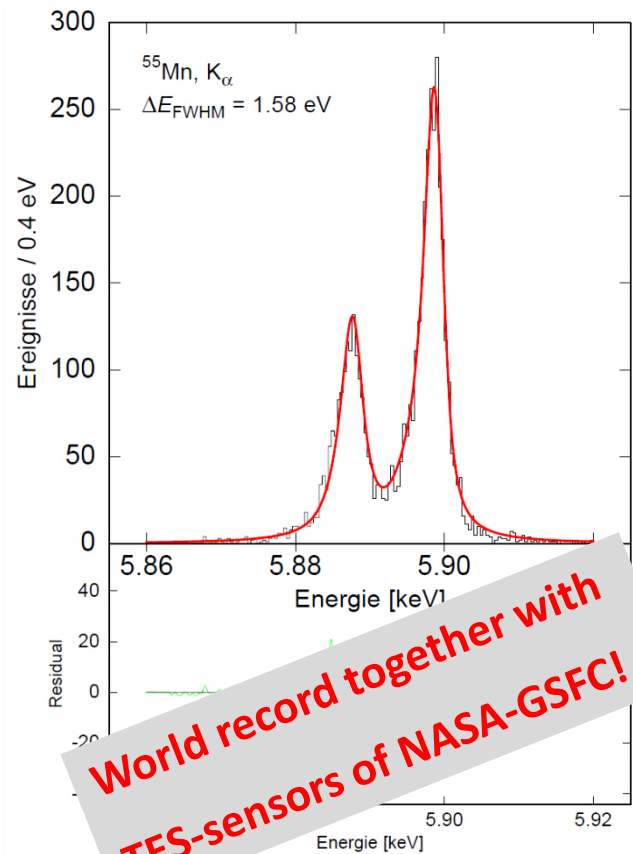
Non-Linearity < 1% @6keV



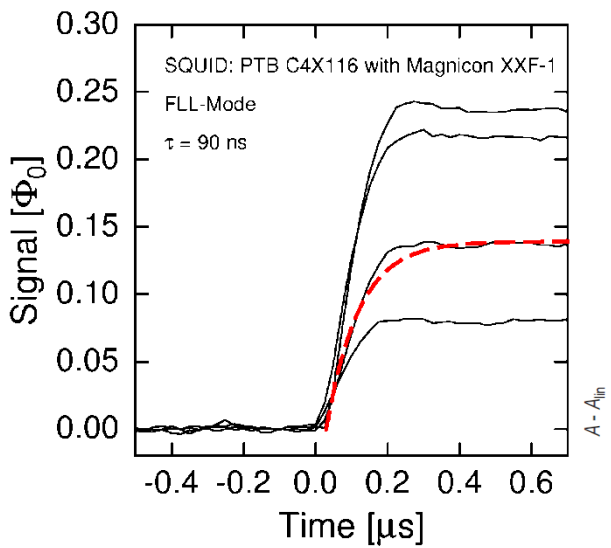
maXs: 1d-array for soft x-rays ($T=20$ mK)



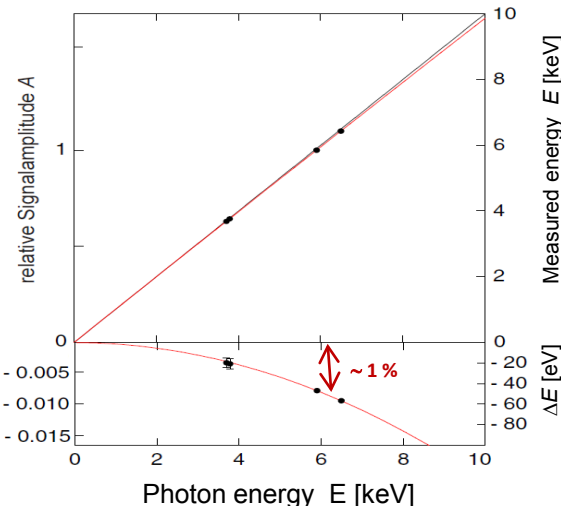
$\Delta E_{FWHM} = 1.6$ eV @ 6 keV



Rise Time: 90 ns

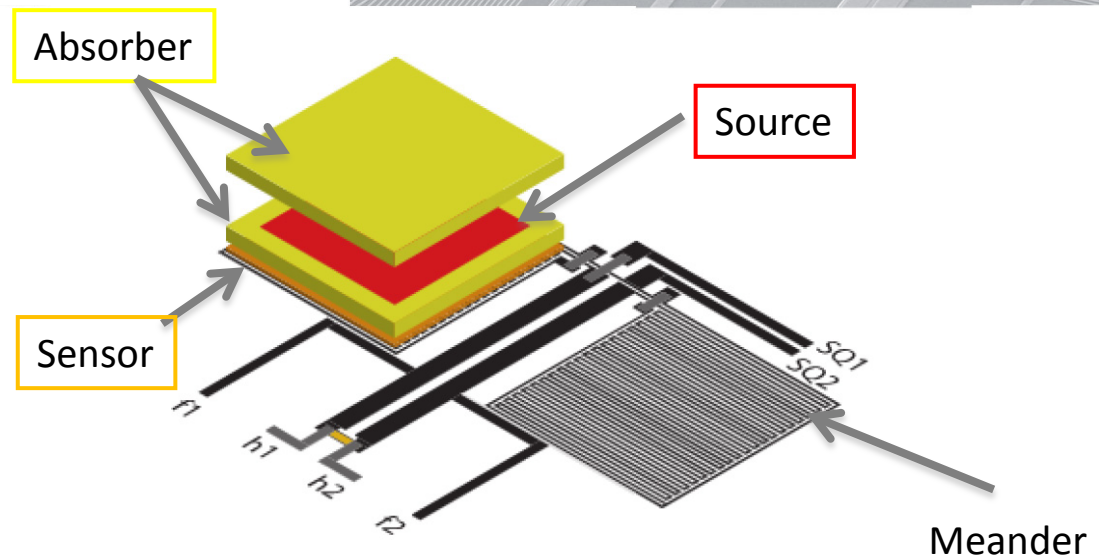
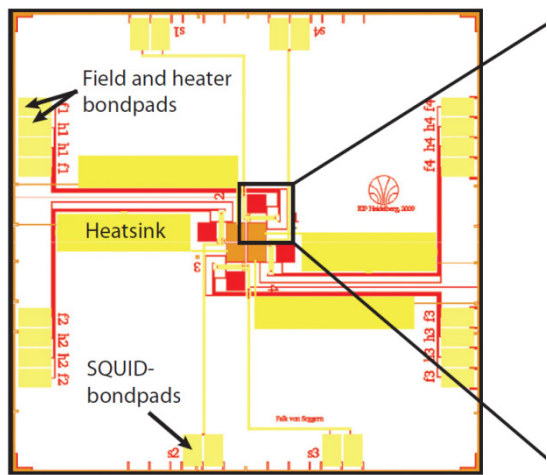
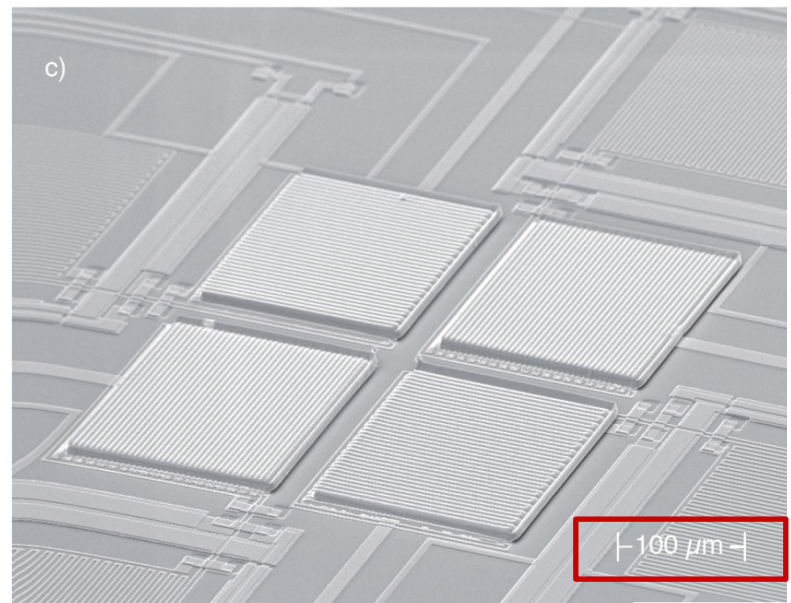


Non-Linearity < 1% @6keV

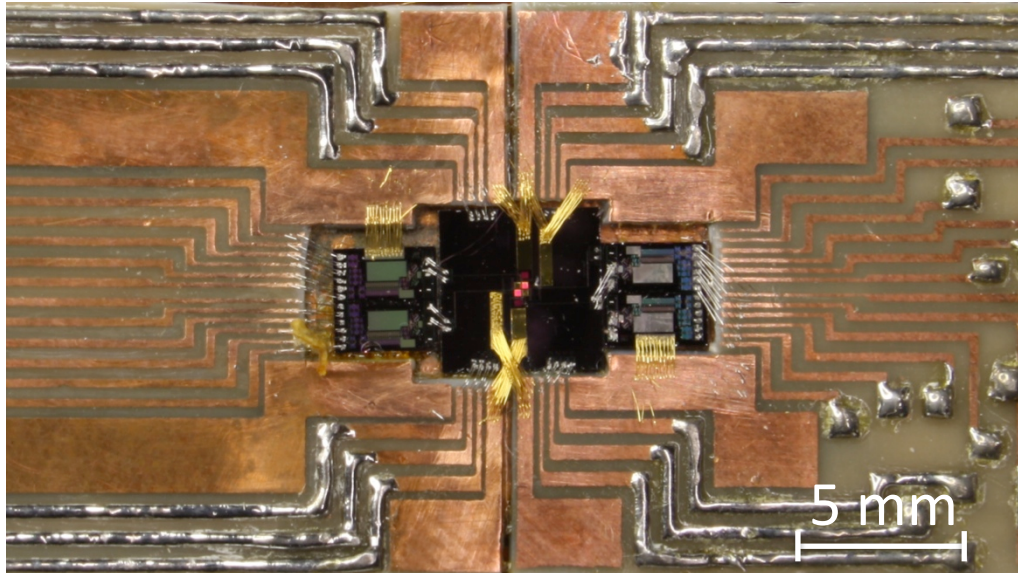


^{163}Ho Detector: First prototype

- Absorber for calorimetric measurement → ion implantation @ ISOLDE-CERN
- Two pixels have been simultaneously measured
- ^{55}Fe calibration source was collimated only on one pixel

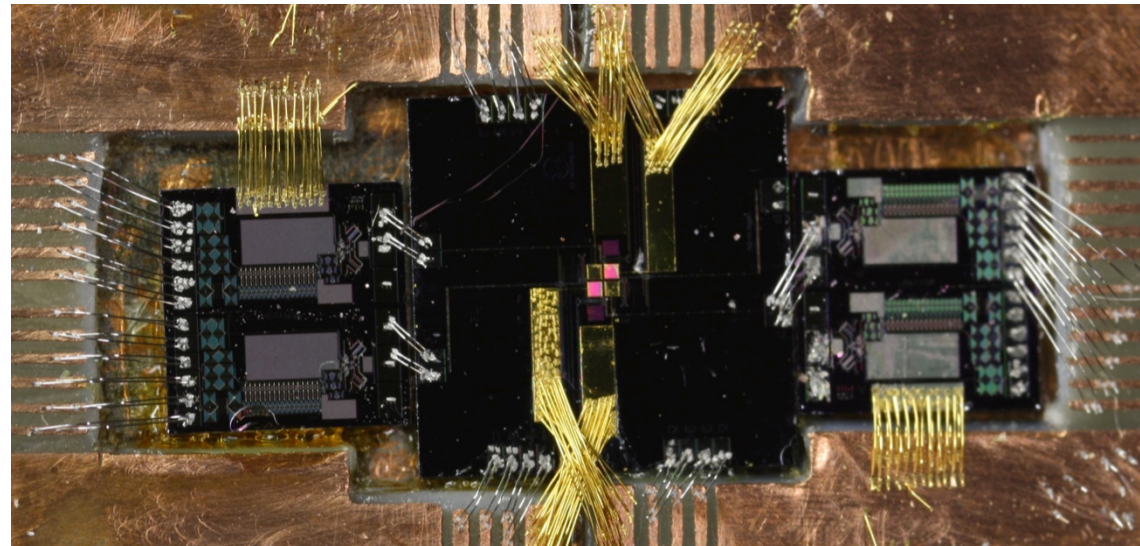


^{163}Ho Detector: First prototype

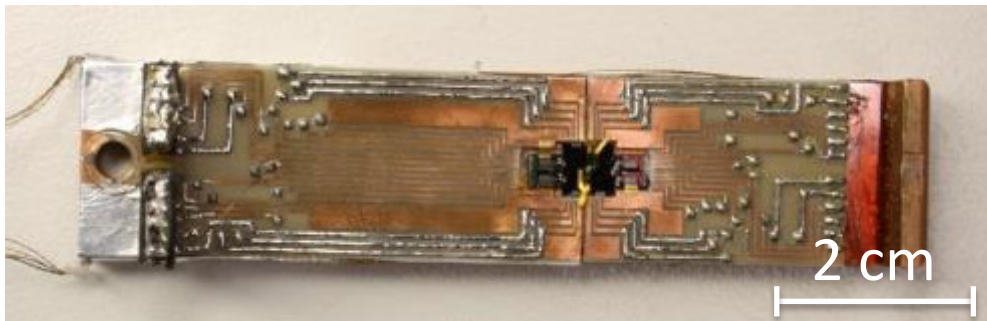


- Newest generation C6X114W SQUIDs (PTB Berlin)
→ best noise performance

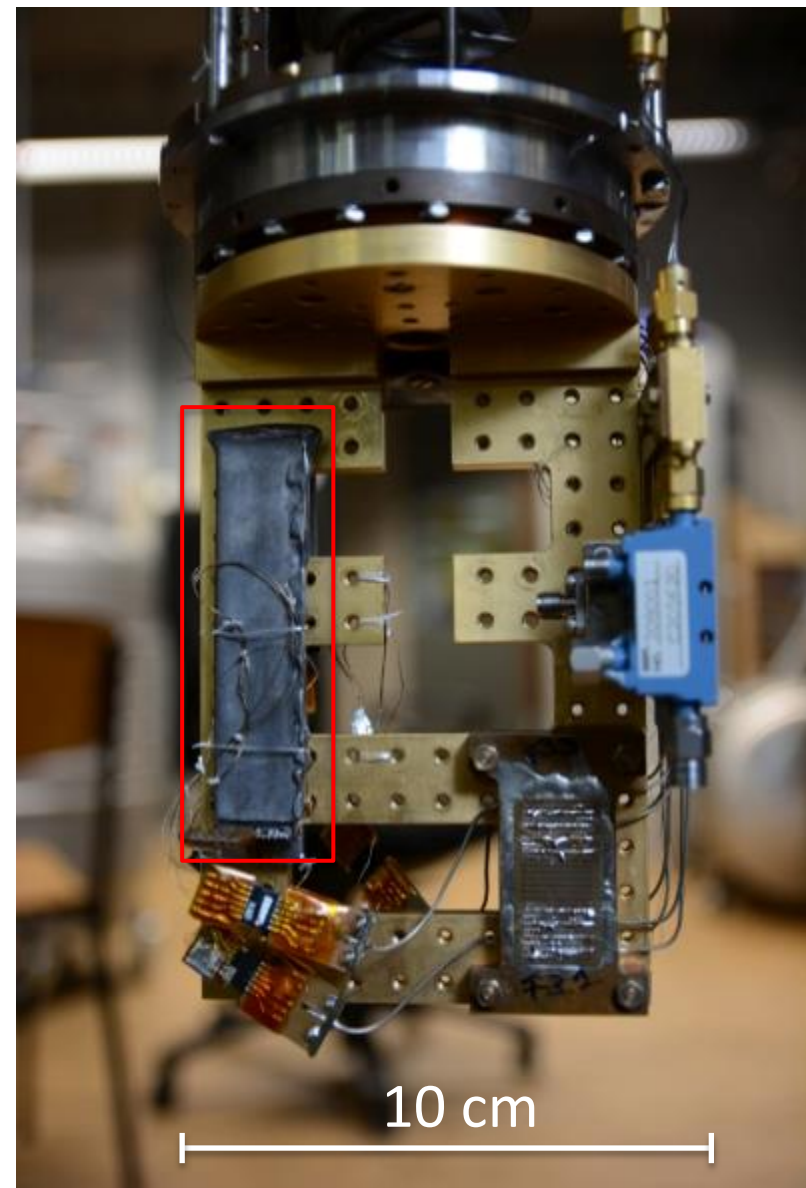
- Al bonding wires for electrical connections
- Au bonding wires for thermal connections



^{163}Ho Detector: Experimental environment



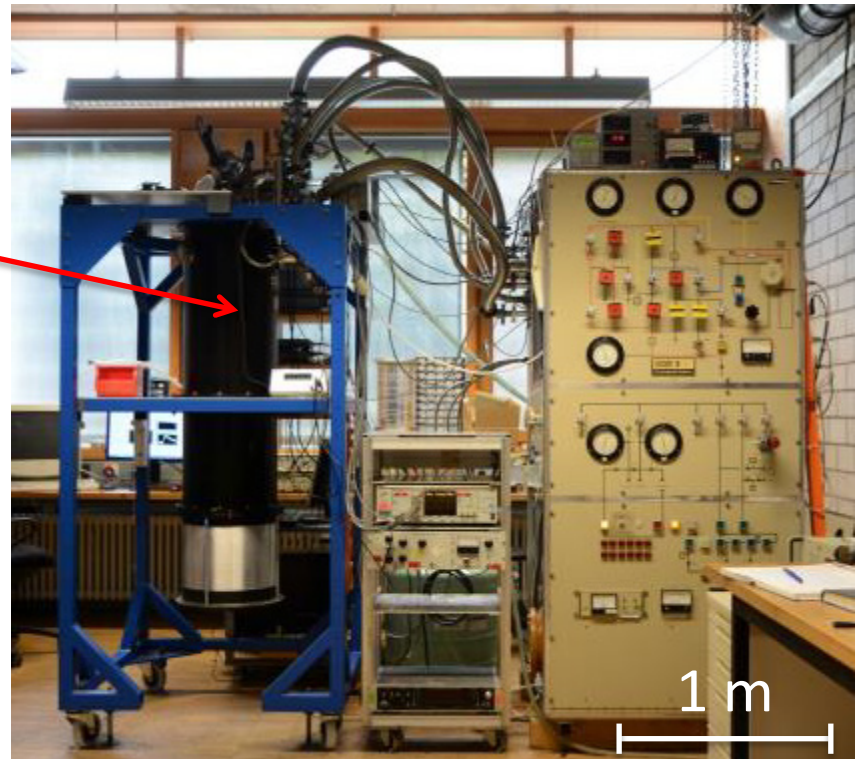
- Cu holder
 - CuFlon circuit board
 - Pb shielding
-
- $^3\text{He}/^4\text{He}$ dilution refrigerator
(Oxford instruments)
 - Cu experimental platform
(Au plated)
 - $T \approx 20 \text{ mK}$



^{163}Ho Detector: Experimental environment

Layered precooling:

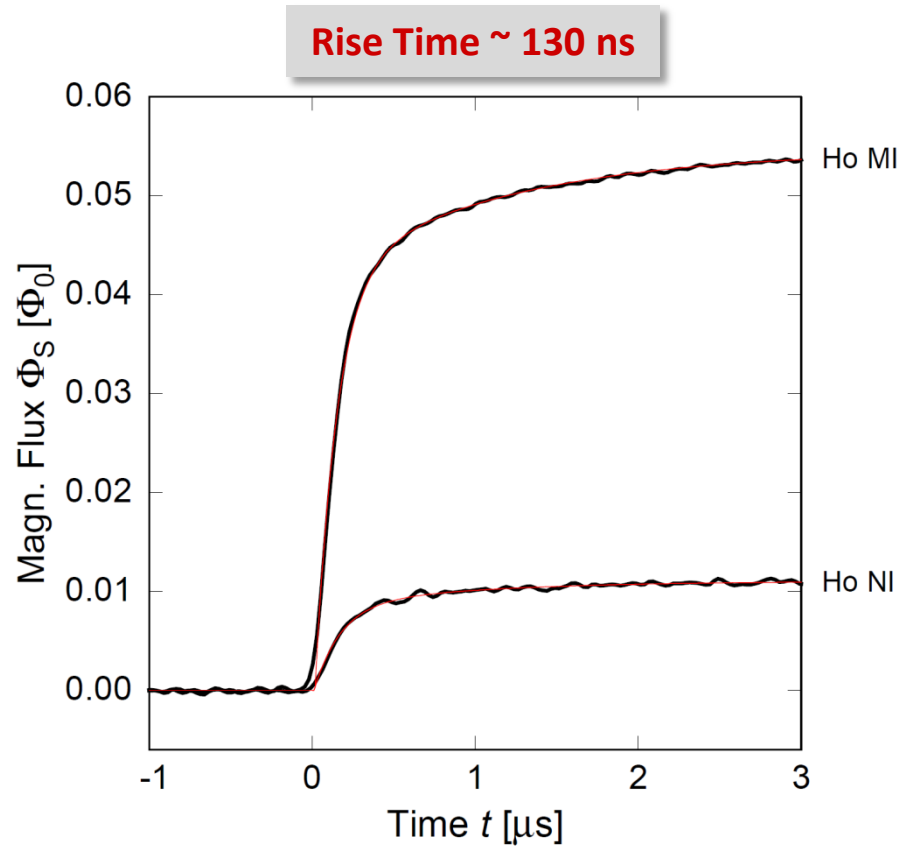
- Liquid $\text{N}_2 \sim 77 \text{ K}$
- Liquid $^4\text{He} \sim 4.2 \text{ K}$



Dilution unit

- 1st stage $\sim 1.5 \text{ K}$
- 2nd stage $\sim 0.6 \text{ K}$
- Experimental platform $\sim 20 \text{ mK}$

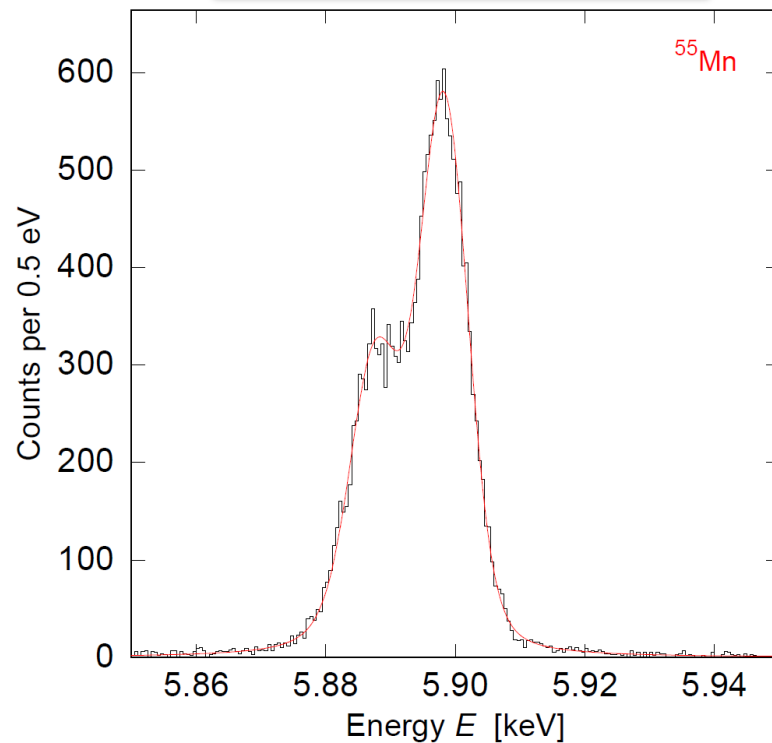
^{163}Ho Detector: Calorimetric spectrum



^{163}Ho Detector: Calorimetric spectrum

- Rise Time ~ 130 ns

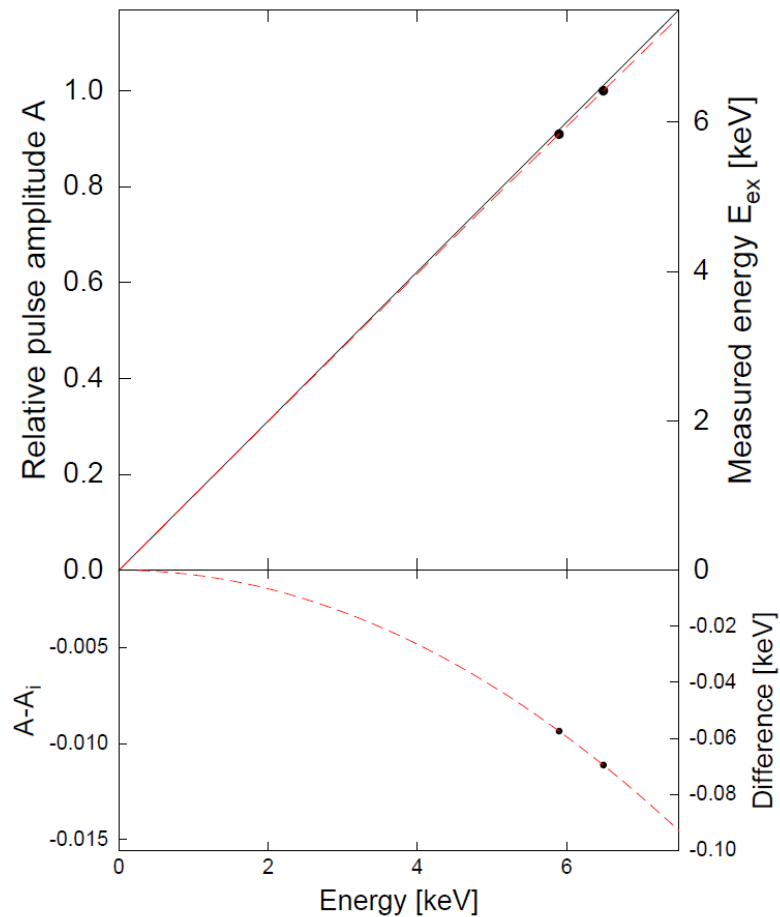
$$\Delta E_{\text{FWHM}} = 7.6 \text{ eV} @ 6 \text{ keV}$$



^{163}Ho Detector: Calorimetric spectrum

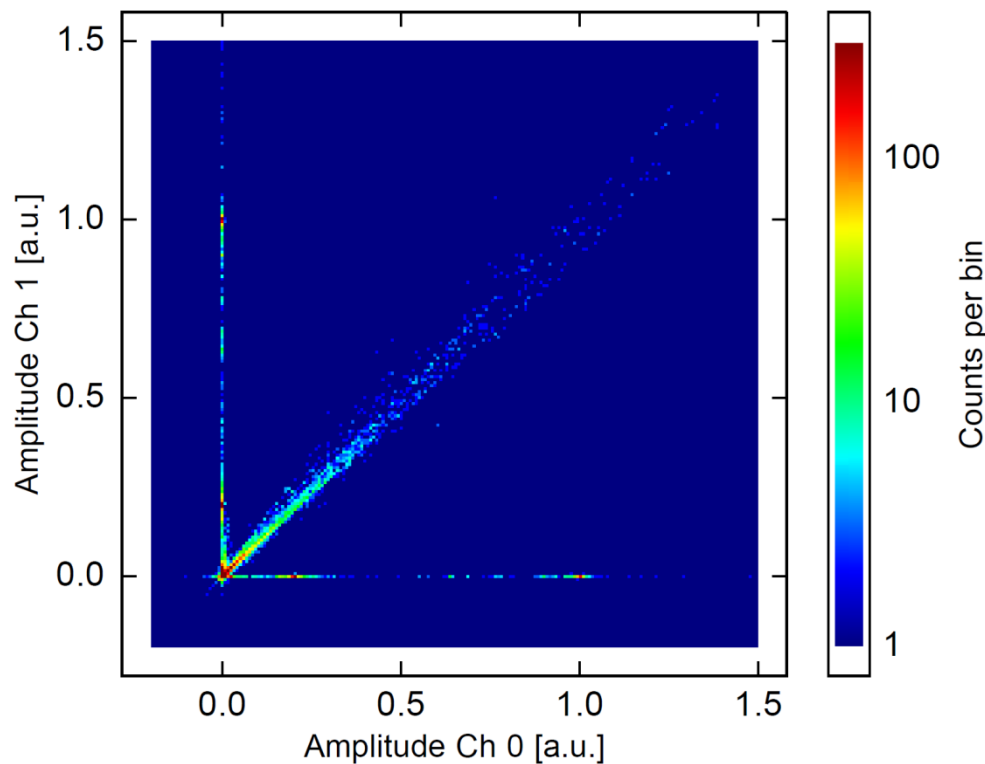
- Rise Time ~ 130 ns
- $\Delta E_{\text{FWHM}} = 7.6$ eV @ 6 keV

Non-Linearity < 1% @6keV



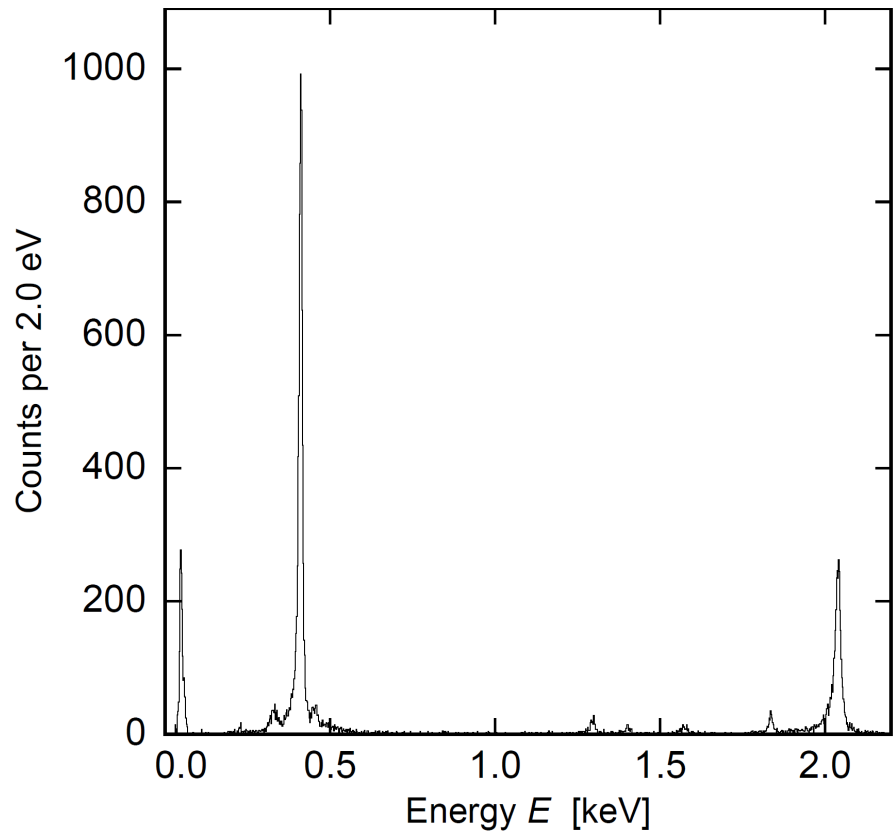
^{163}Ho Detector: Calorimetric spectrum

- Rise Time ~ 130 ns
- $\Delta E_{\text{FWHM}} = 7.6$ eV @ 6 keV
- Non-Linearity < 1% @6keV



^{163}Ho Detector: Calorimetric spectrum

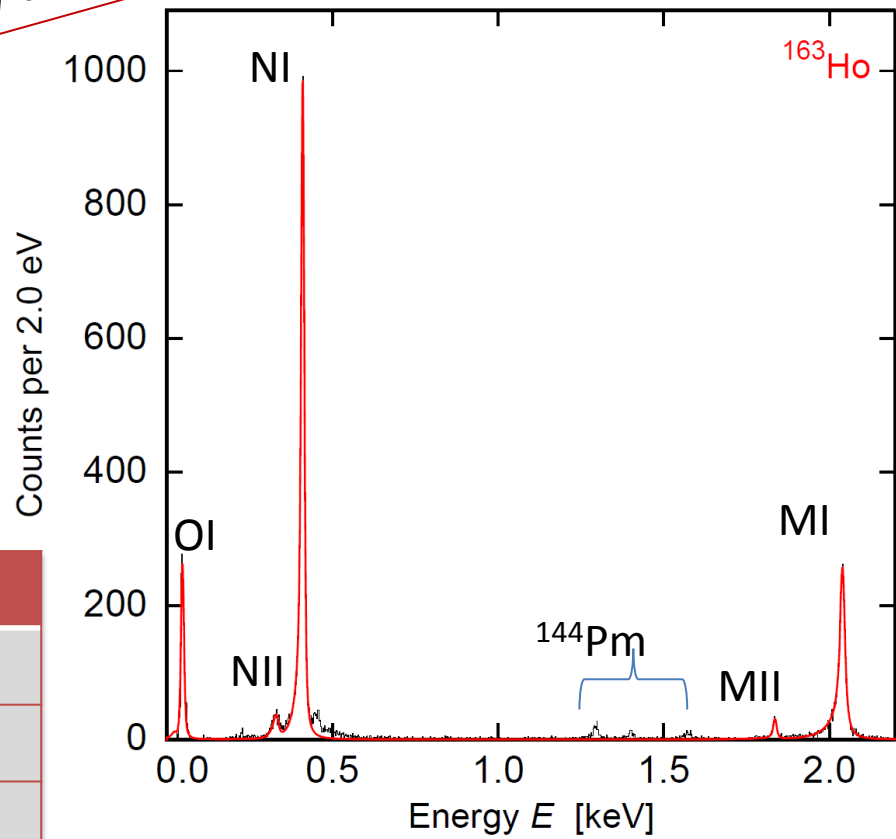
- Rise Time ~ 130 ns
- $\Delta E_{\text{FWHM}} = 7.6$ eV @ 6 keV
- Non-Linearity < 1% @6keV



^{163}Ho Detector: Calorimetric spectrum

- Rise Time ~ 130 ns
- $\Delta E_{\text{FWHM}} = 7.6$ eV @ 6 keV
- Non-Linearity < 1% @ 6keV
- Most precise ^{163}Ho spectrum

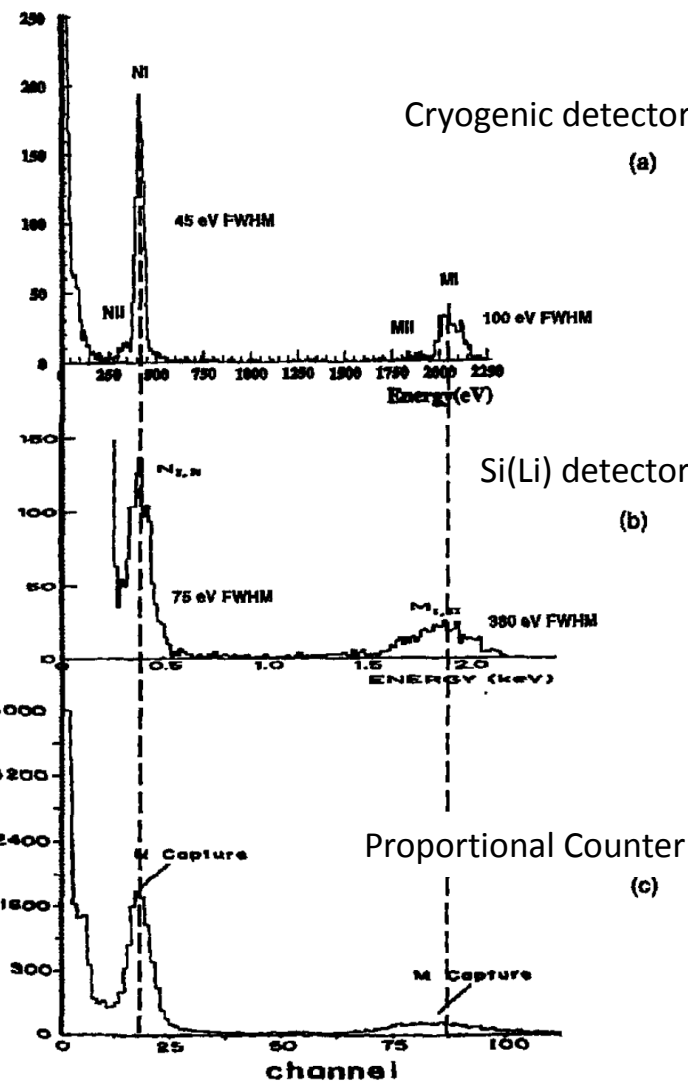
Preliminary analysis



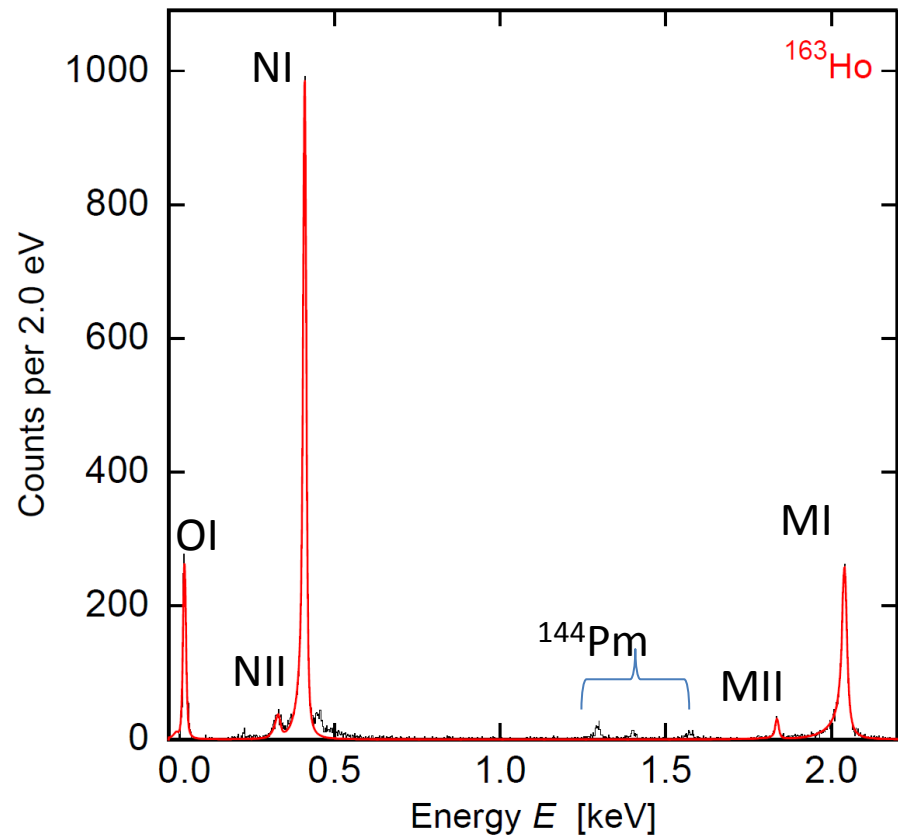
	E_H lit.	E_H exp.	Γ_H lit.	Γ_H exp
MI	2.047	2.040	13.2	13.7
MII	1.845	1.836	6.0	7.2
NI	0.420	0.411	5.4	5.3
NII	0.340	0.333	5.3	8.0
OI	0.050	0.048	5.0	4.3

$$Q_{\text{EC}} = (2.80 \pm 0.08) \text{ keV}$$

^{163}Ho Detector: Calorimetric spectrum

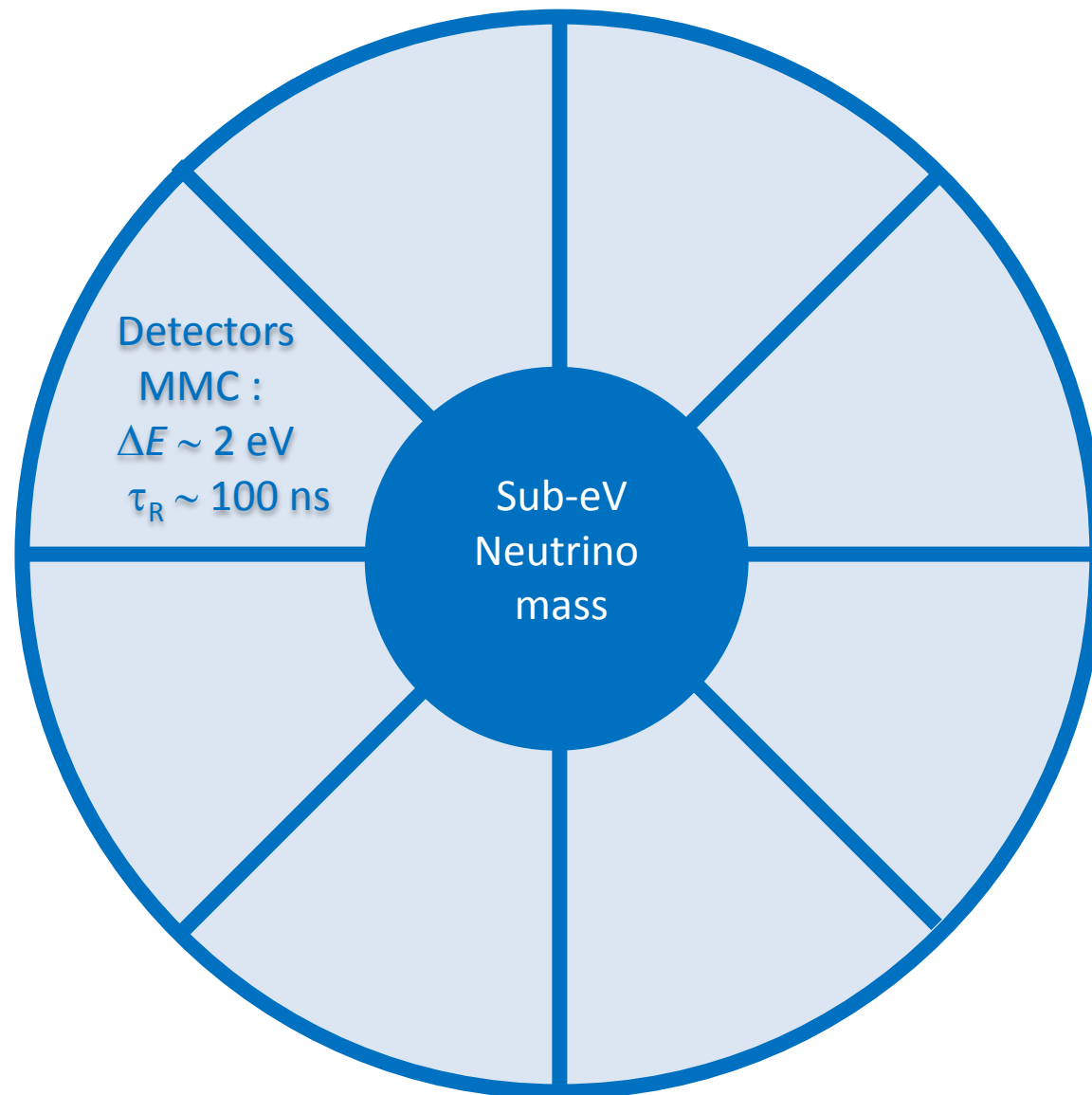


F. Gatti et al., Physics Letters B 398 (1997) 415-419

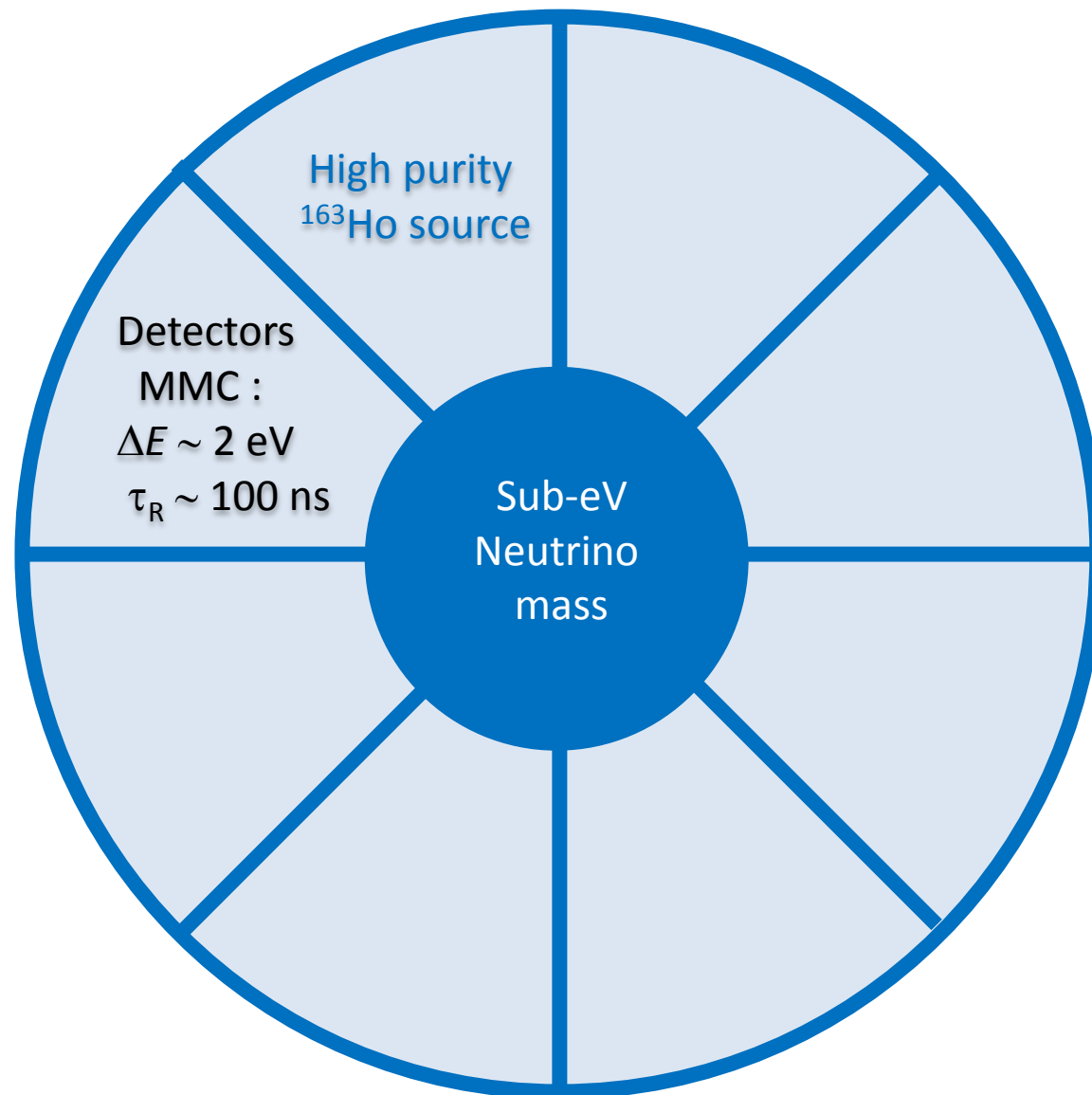


- (a) F. Gatti et al., Physics Letters B 398 (1997) 415-419
- (b) E. Laesgaard et al., Proceeding of 7th International Conference on Atomic Masses and Fundamental Constants (AMCO-7), (1984).
- (c) F.X. Hartmann and R.A. Naumann, Nucl. Instr. Meth. A 3 13 (1992) 237.

ECHo experiment



ECHo experiment



ECHo experiment: ^{163}Ho source

- Required activity in the detectors: Final experiment $\rightarrow >10^6 \text{ Bq} \rightarrow >10^{17} \text{ atoms}$

ECHo experiment: ^{163}Ho source

- Required activity in the detectors: Final experiment $\rightarrow >10^6 \text{ Bq} \rightarrow >10^{17} \text{ atoms}$
- ^{163}Ho can be produced by charged particle activation through direct or indirect way
 - $^{nat}\text{Dy}(p, xn) ^{163}\text{Ho}$
 - $^{nat}\text{Dy}(\alpha, xn) ^{163}\text{Er} (\varepsilon) ^{163}\text{Ho}$
 - $^{159}\text{Tb}(^7\text{Li}, 3n) ^{163}\text{Er} (\varepsilon) ^{163}\text{Ho}$

Er155 5.3 m 7/2-	Er156 19.5 m 0+	Er157 18.65 m 3/2- *	Er158 2.29 h 0+	Er159 36 m 3/2-	Er160 28.58 h 0+	Er161 3.21 h 3/2-	Er162 0+	Er163 75.0 m 5/2-	Er164 0+	Er165 10.36 h 5/2-	Er166 0+
C, α	EC	EC	EC	EC	EC	EC	0.14	EC	1.61	EC	33.6
Ho154 11.76 m (2)- *	Ho155 48 m 5/2+	Ho156 56 m (4+)*	Ho157 12.6 m 7/2-	Ho158 11.3 m 5+ *	Ho159 33.05 m 7/2- *	Ho160 25.6 m 5+ *	Ho161 2.48 h 7/2- *	Ho162 15.0 m 1+ *	Ho163 4570 y 7/2- *	Ho164 29 m 1+ *	Ho165 7/2- *
C, α	EC	EC	EC	EC	EC	EC	EC	EC	EC	EC, β -	100
Dy153 6.4 h 7/2(-)	Dy154 3.0E+6 y 0+	Dy155 9.9 h 3/2-	Dy156 0+	Dy157 8.14 h 3/2- *	Dy158 0+	Dy159 144.4 d 3/2-	Dy160 0+	Dy161 5/2+	Dy162 0+	Dy163 5/2-	Dy164 0+
			α	EC	0.06	EC	0.10	EC	2.34	18.9	25.5
Tb152 17.5 h 2- *	Tb153 2.34 d 5/2+	Tb154 21.5 h 0 *	Tb155 5.32 d 3/2+	Tb156 5.35 d 3- *	Tb157 71 y 3/2+	Tb158 180 y 3- *	Tb159 3/2+	Tb160 72.3 d 3-	Tb161 6.88 d 3/2+	Tb162 7.60 m 1-	Tb163 19.5 m 3/2+
C, α	EC	EC, β -	EC	EC, β -	EC	EC, β -	100	β -	β -	β -	β -

ECHo experiment: ^{163}Ho source

- Required activity in the detectors: Final experiment $\rightarrow >10^6 \text{ Bq} \rightarrow >10^{17} \text{ atoms}$
- \triangleright ^{163}Ho can be produced by charged particle activation through direct or indirect way
 - $^{nat}\text{Dy}(p, xn) ^{163}\text{Ho}$
 - $^{nat}\text{Dy}(\alpha, xn) ^{163}\text{Er} (\varepsilon) ^{163}\text{Ho}$
 - $^{159}\text{Tb}(^7\text{Li}, 3n) ^{163}\text{Er} (\varepsilon) ^{163}\text{Ho}$
- \triangleright ^{163}Ho can be produced by via (n, γ) -reaction on ^{162}Er

Er155 5.3 m 7/2-	Er156 19.5 m 0+	Er157 18.65 m 3/2- *	Er158 2.29 h 0+	Er159 36 m 3/2-	Er160 28.58 h 0+	Er161 3.21 h 3/2-	Er162 0+	Er163 75.0 m 5/2-	Er164 0+	Er165 10.36 h 5/2-	Er166 0+
C, α	EC	EC	EC	EC	EC	EC	0.14	EC	1.61	EC	33.6
Ho154 11.76 m (2)- *	Ho155 48 m 5/2+	Ho156 56 m (4+) *	Ho157 12.6 m 7/2-	Ho158 11.3 m 5+ *	Ho159 33.05 m 7/2- *	Ho160 25.6 m 5+ *	Ho161 2.48 h 7/2- *	Ho162 15.0 m 1+ *	Ho163 4570 y 7/2- *	Ho164 29 m 1+ *	Ho165 7/2- *
C, α	EC	EC	EC	EC	EC	EC	EC	EC	EC	EC, β^-	100
Dy153 6.4 h 7/2(-)	Dy154 3.0E+6 y 0+	Dy155 9.9 h 3/2-	Dy156 0+	Dy157 8.14 h 3/2- *	Dy158 0+	Dy159 144.4 d 3/2-	Dy160 0+	Dy161 5/2+	Dy162 0+	Dy163 5/2-	Dy164 0+
			α	EC	0.06	EC	0.10	EC	2.34	18.9	25.5
Tb152 17.5 h 2- *	Tb153 2.34 d 5/2+	Tb154 21.5 h 0 *	Tb155 5.32 d 3/2+	Tb156 5.35 d 3- *	Tb157 71 y 3/2+	Tb158 180 y 3- *	Tb159 3/2+	Tb160 72.3 d 3-	Tb161 6.88 d 3/2+	Tb162 7.60 m 1-	Tb163 19.5 m 3/2+
C, α	EC	EC, β^-	EC	EC, β^-	EC	EC, β^-	100	β^-	β^-	β^-	β^-

ECHo experiment: ^{163}Ho source

- Required activity in the detectors: Final experiment $\rightarrow >10^6 \text{ Bq} \rightarrow >10^{17}$ atoms
- ^{163}Ho can be produced by charged particle activation through direct or indirect way
 - $^{\text{nat}}\text{Dy}(\text{p}, \text{xn}) \ ^{163}\text{Ho}$
 - $^{\text{nat}}\text{Dy}(\alpha, \text{xn}) \ ^{163}\text{Er} (\varepsilon) \ ^{163}\text{Ho}$
 - $^{159}\text{Tb}(\text{Li}, \text{3n}) \ ^{163}\text{Er} (\varepsilon) \ ^{163}\text{Ho}$
- ^{163}Ho can be produced by via (n, γ) -reaction on ^{162}Er

Two sources already produced

- ✓ Helmholtz Zentrum Berlin
- ✓ Institut Laue-Langevin in Grenoble

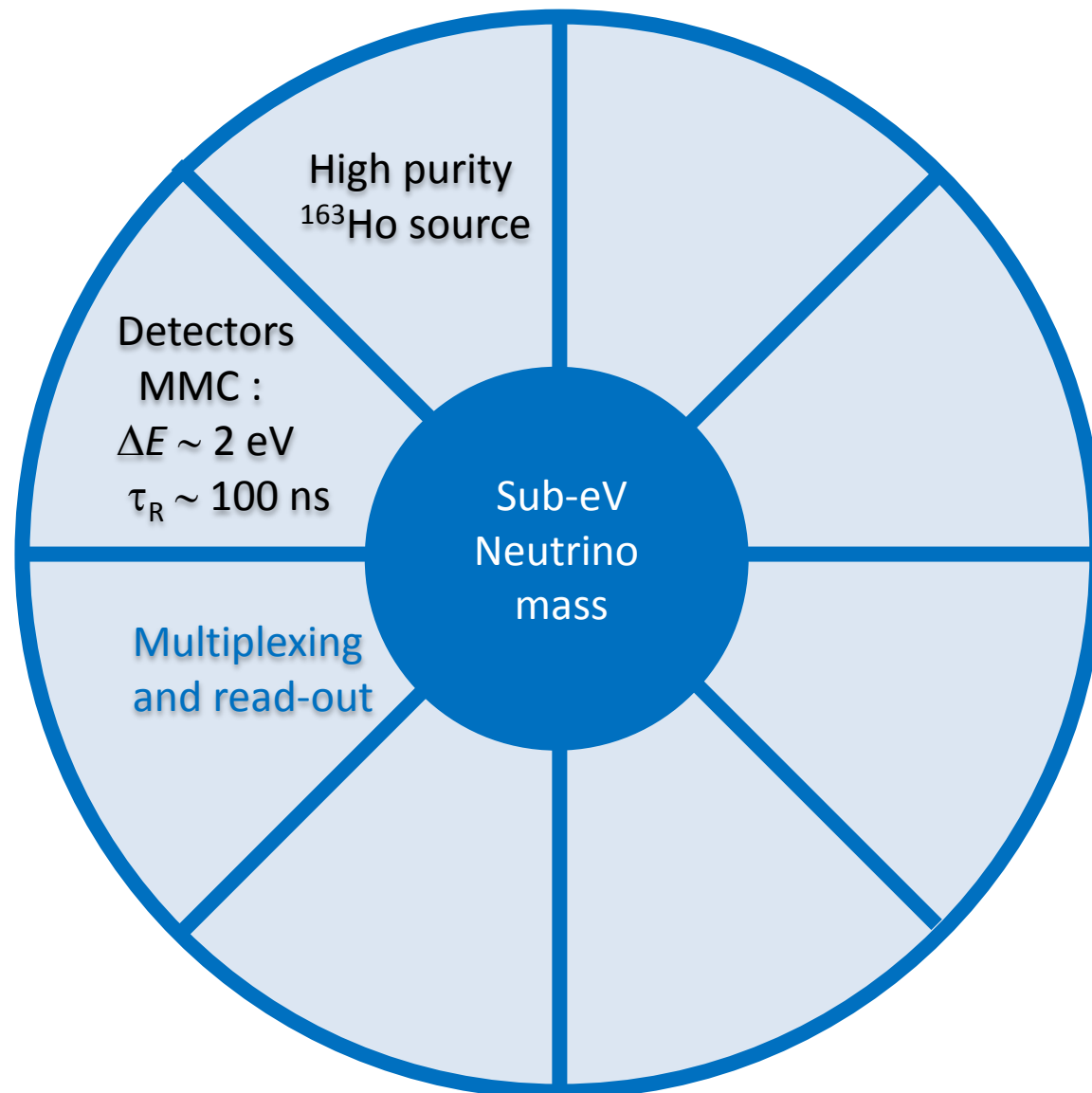
ECHo experiment: ^{163}Ho source

- Required activity in the detectors: Final experiment $\rightarrow >10^6 \text{ Bq} \rightarrow >10^{17}$ atoms
- ^{163}Ho can be produced by charged particle activation through direct or indirect way
 - $^{\text{nat}}\text{Dy}(\text{p}, \text{xn}) ^{163}\text{Ho}$
 - $^{\text{nat}}\text{Dy}(\alpha, \text{xn}) ^{163}\text{Er} (\varepsilon) ^{163}\text{Ho}$
 - $^{159}\text{Tb}({}^7\text{Li}, 3\text{n}) ^{163}\text{Er} (\varepsilon) ^{163}\text{Ho}$
- ^{163}Ho can be produced by via (n, γ) -reaction on ^{162}Er

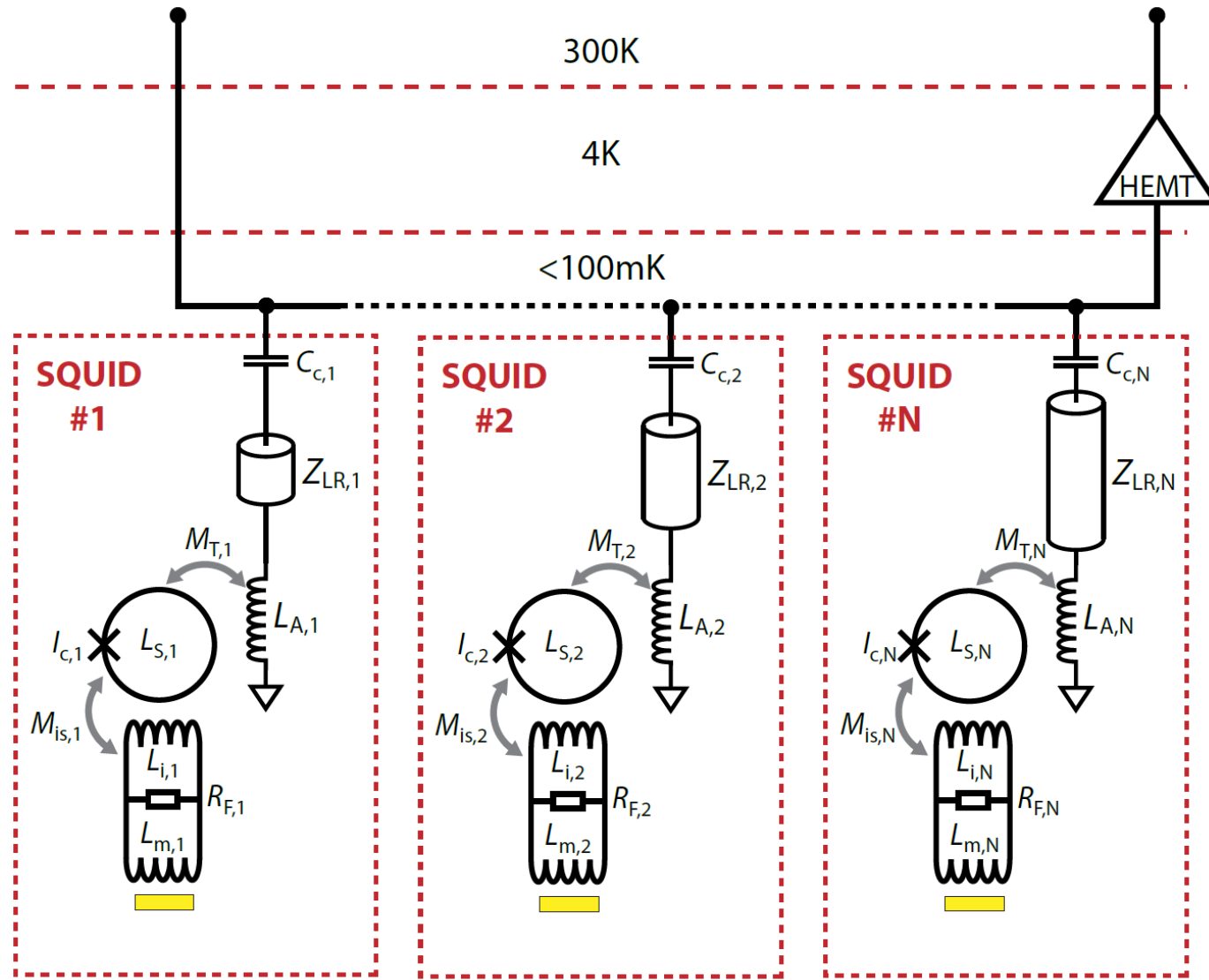
Two sources already produced

 - ✓ Helmholtz Zentrum Berlin
 - ✓ Institut Laue-Langevin in Grenoble
- Purity: No radioactive contaminants and removed target material
- High efficiency purification methods
- Chemical form: depends on the absorber preparation (ion implantation, dilute alloys)

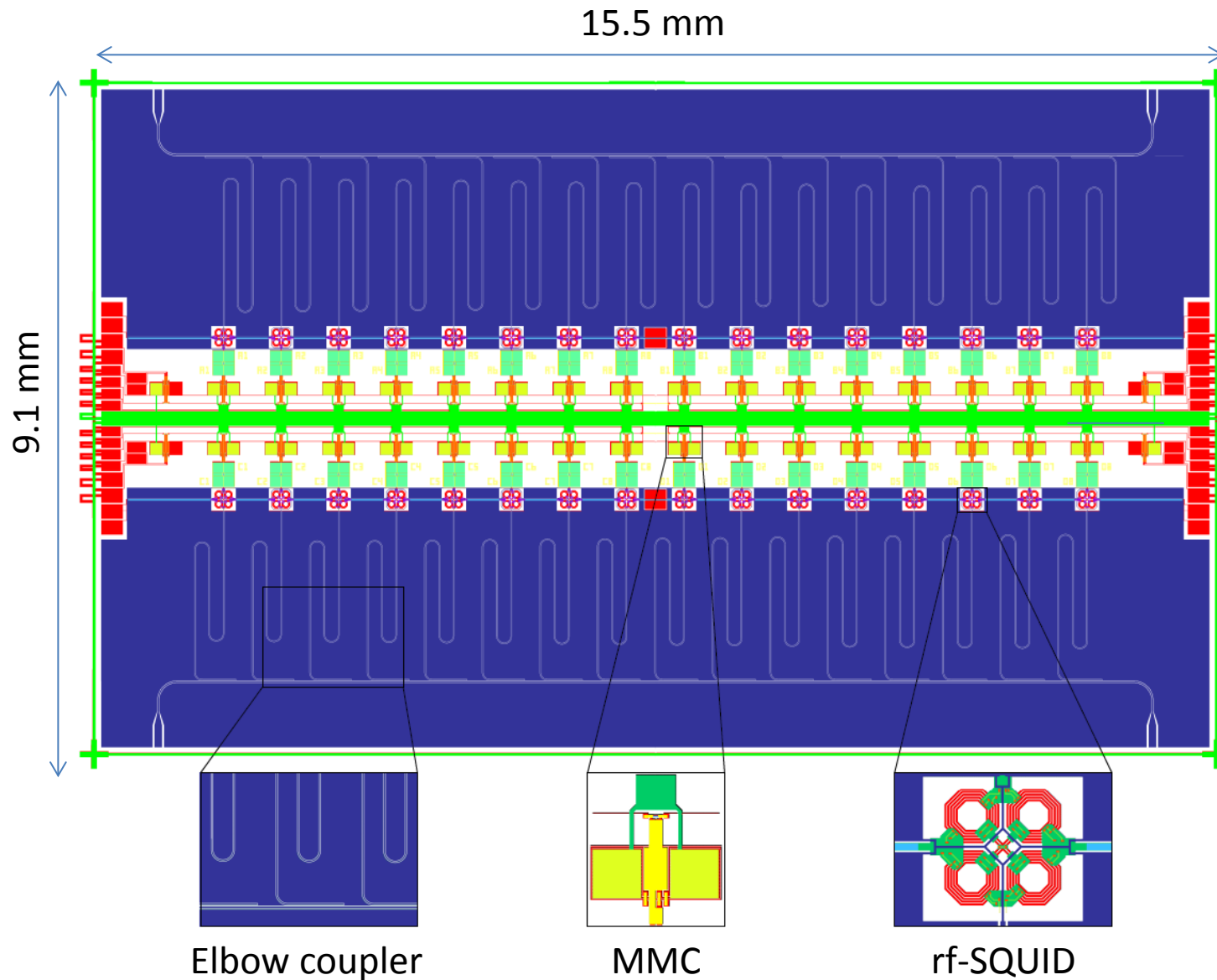
ECHo experiment



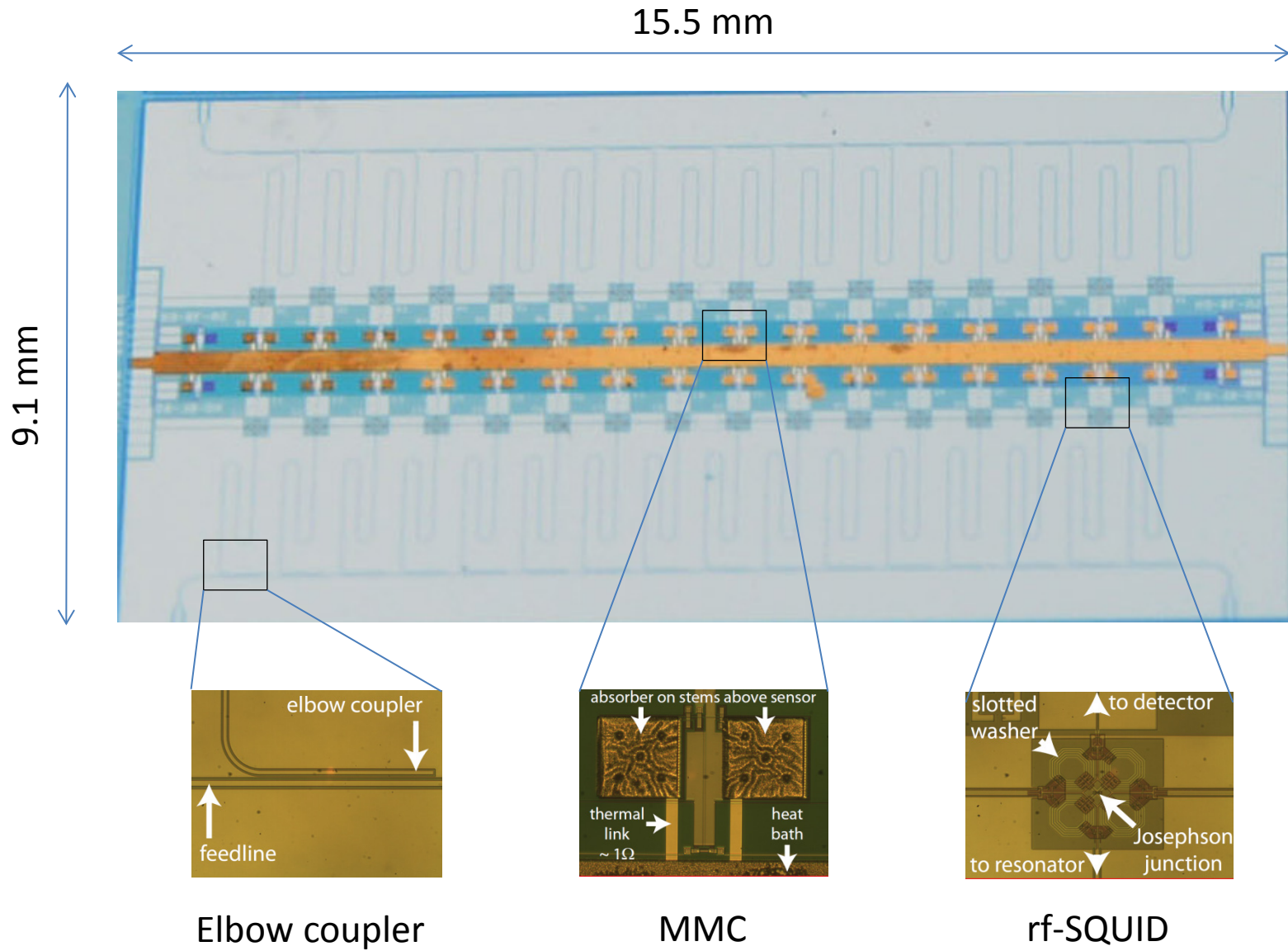
ECHo experiment: μwave SQUID multiplexing



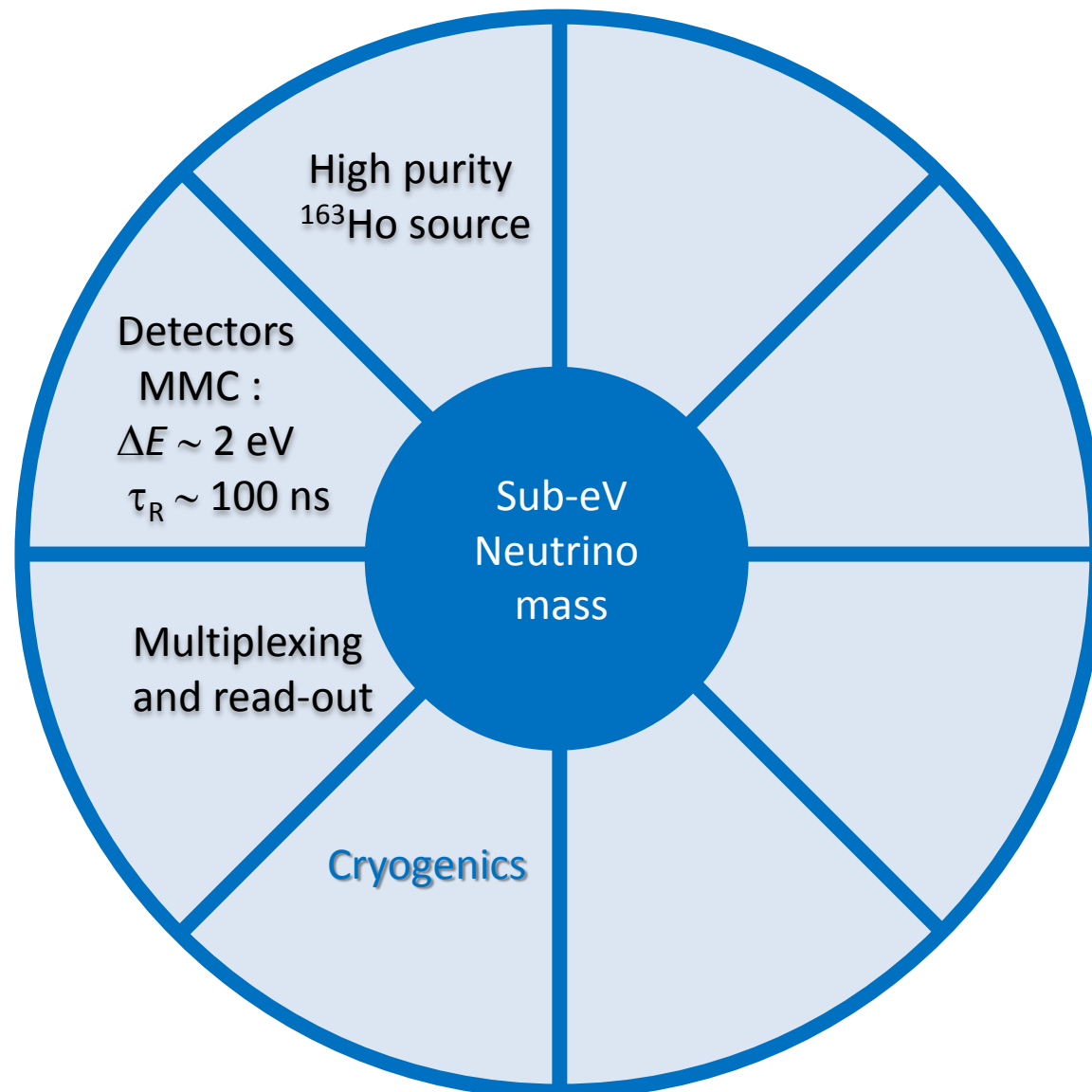
ECHo experiment: 64-pixel chip



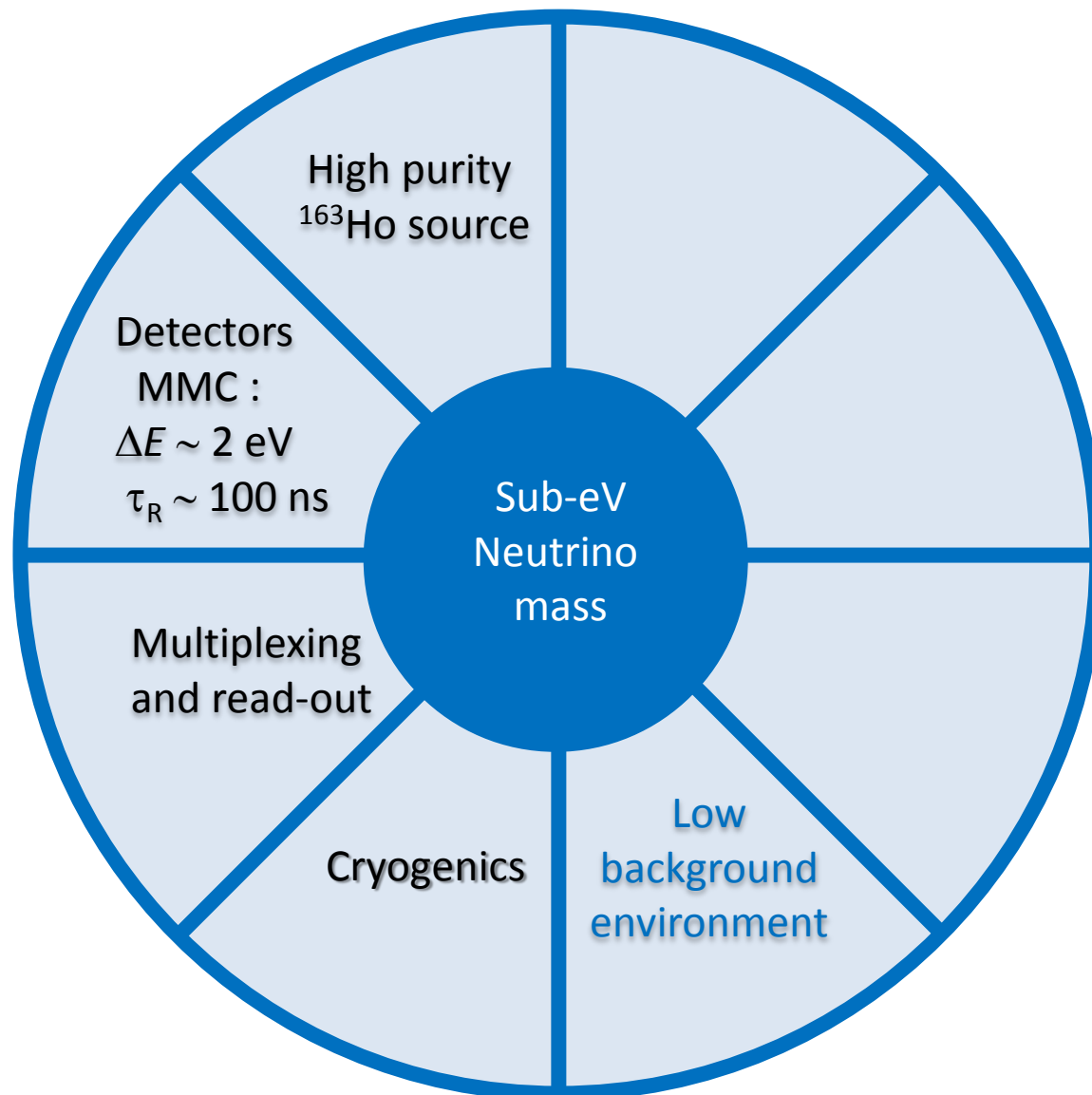
ECHo experiment: 64-pixel chip



ECHo experiment



ECHo experiment



ECHo experiment: Low background

Background sources:

- Contamination of the source → ^{166m}Ho
- Environmental radioactivity
- Induced secondary radiation by cosmic rays



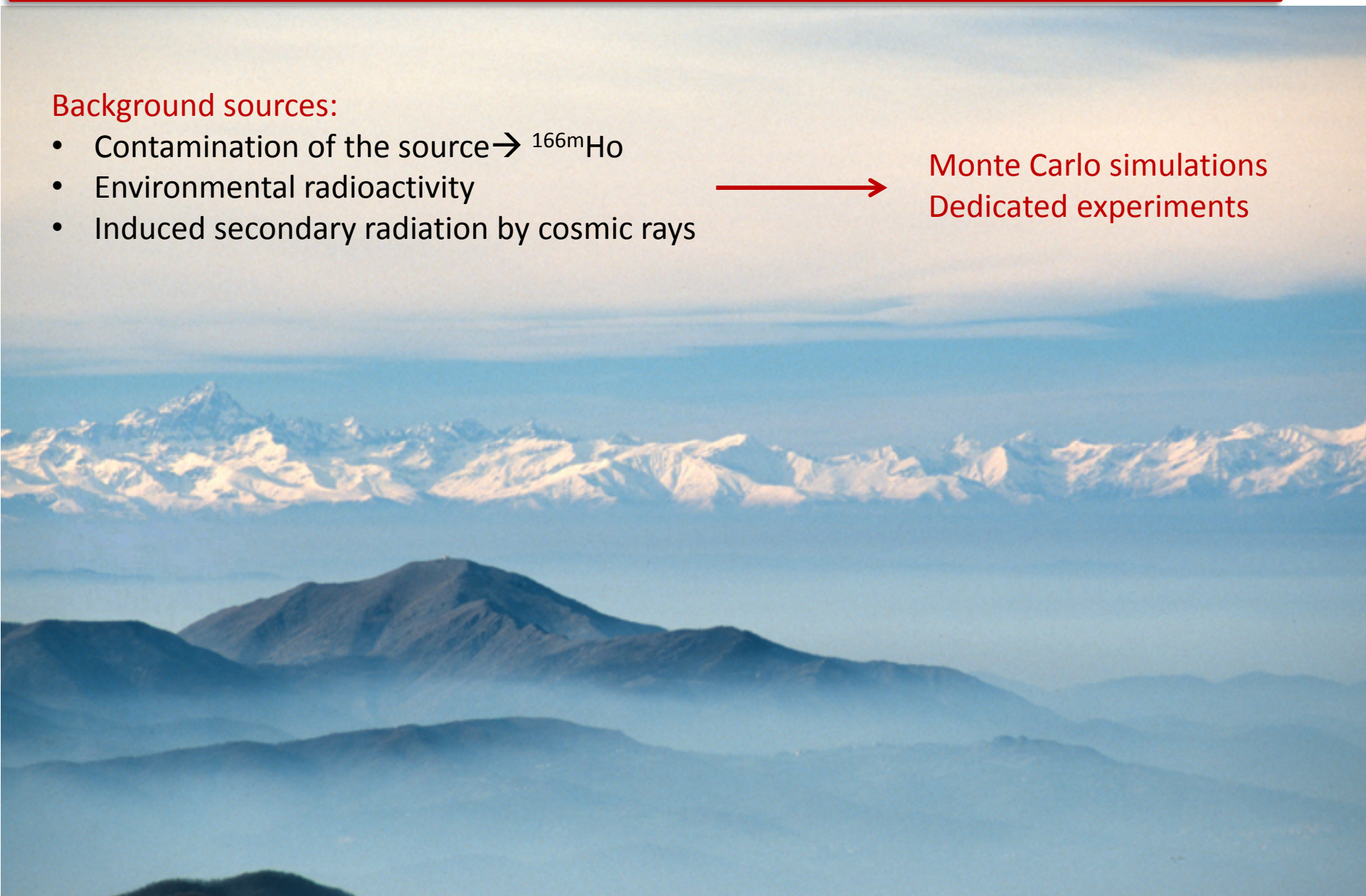
ECHo experiment: Low background

Background sources:

- Contamination of the source → ^{166m}Ho
- Environmental radioactivity
- Induced secondary radiation by cosmic rays



Monte Carlo simulations
Dedicated experiments



ECHo experiment: Low background

Background sources:

- Contamination of the source → ^{166m}Ho
- Environmental radioactivity
- Induced secondary radiation by cosmic rays



Monte Carlo simulations
Dedicated experiments

First measurements
underground in Modane
winter 2013

ECHo experiment: Low background

Background sources:

- Contamination of the source → ^{166m}Ho
- Environmental radioactivity
- Induced secondary radiation by cosmic rays

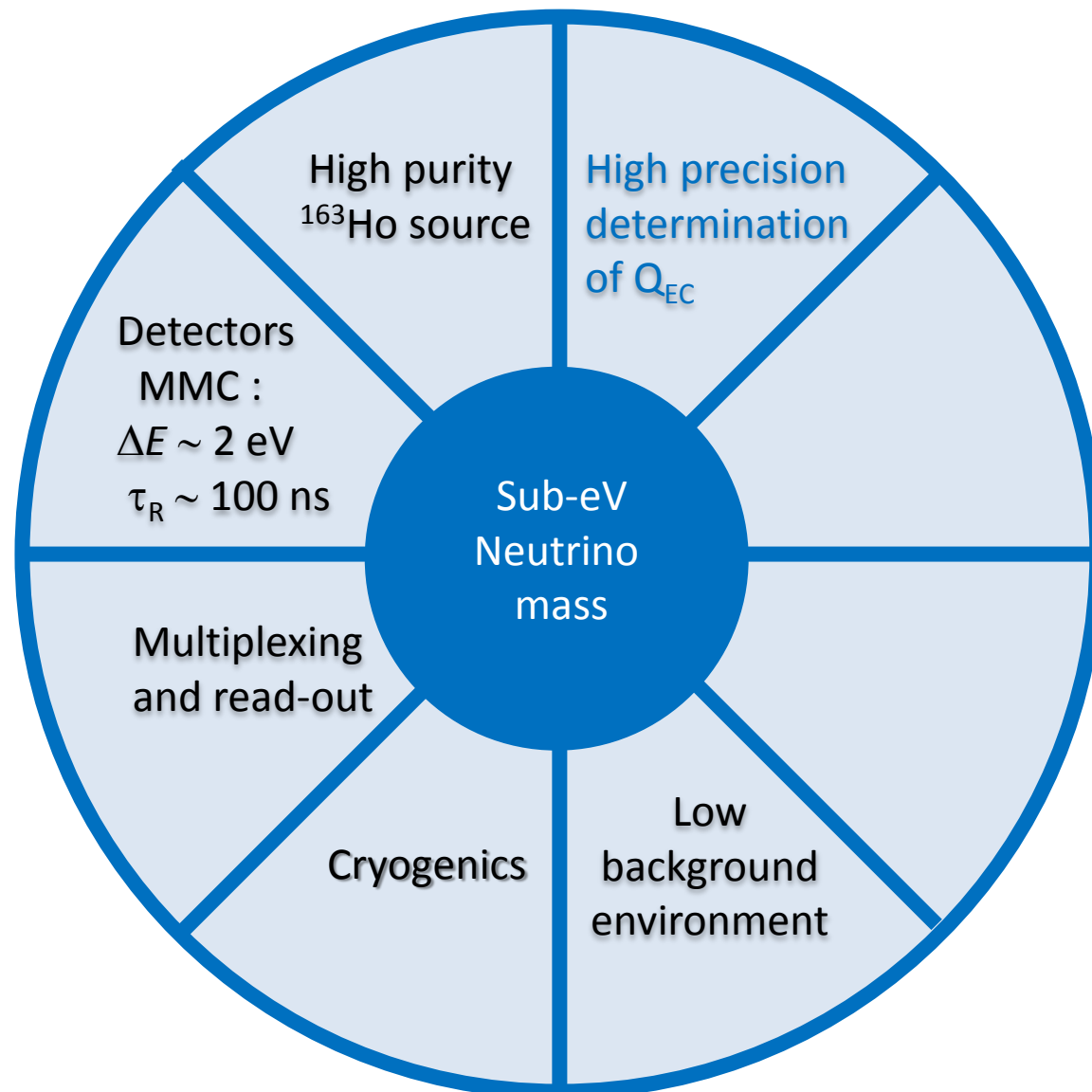


Monte Carlo simulations
Dedicated experiments

First measurements
underground in Modane
winter 2013

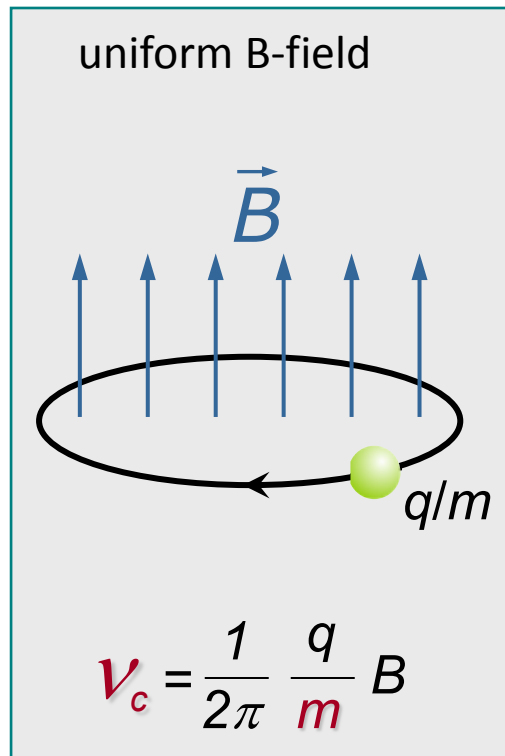
- ✓ Selection of materials for the experimental set-up
- ✓ Definition of detector design → veto
- ✓ Designs for the shielding

ECHo experiment

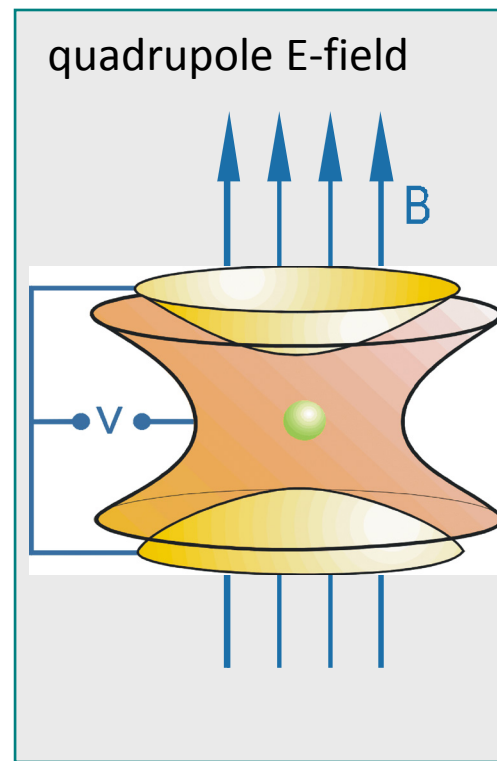


ECHo experiment: Q_{EC} determination

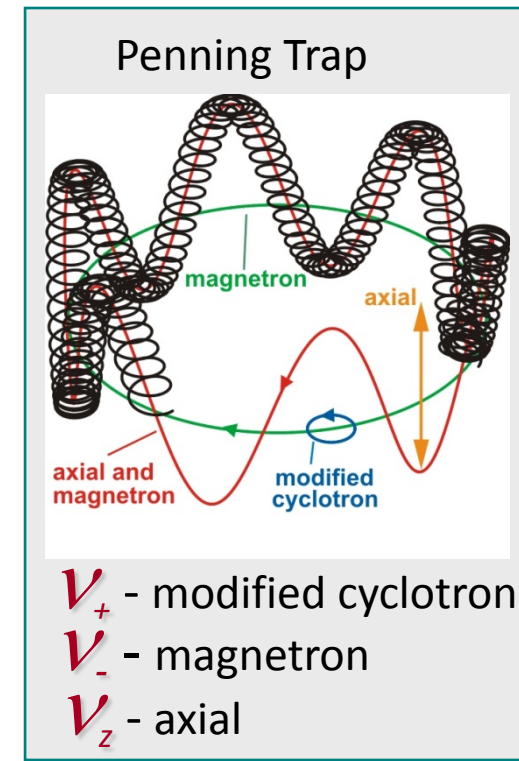
Penning Trap mass spectroscopy



+



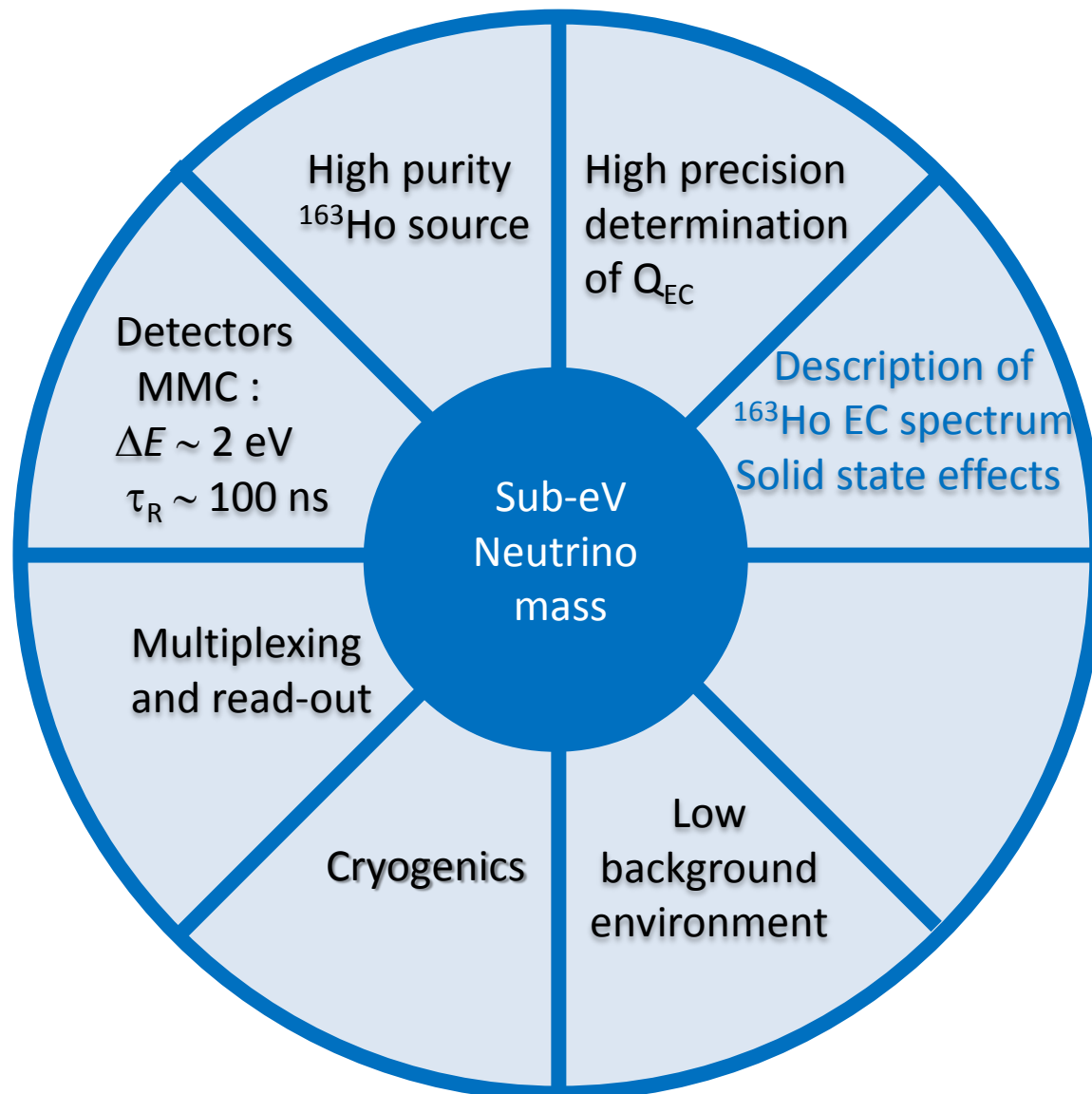
=



Next future : SHIPTRAP (GSI) → Q_{EC} determination within 100 eV

In few years: PENTATRAP (MPI-K HD) → Q_{EC} determination within 1 eV

ECHo experiment



ECHo experiment: spectral shape

How precise do we know the calorimetric spectrum of ^{163}Ho ?

$$\frac{dW}{dE_C} = \boxed{A} (Q_{\text{EC}} - E_C)^2 \sqrt{1 - \frac{m_\nu^2}{(Q_{\text{EC}} - E_C)^2}} \sum_H \boxed{B_H} \boxed{\varphi_H^2(0)} \frac{\boxed{\Gamma_H}}{(E_C - \boxed{E_H})^2 + \frac{\boxed{\Gamma_H}^2}{4}}$$

Density Functional Theory (DFT) & Quasiparticle Random Phase Approximation (QRPA)

SOLID STATE EFFECTS

Experimental investigations:

^{163}Ho implanted in different materials

Simple ^{163}Ho molecules implanted in Au

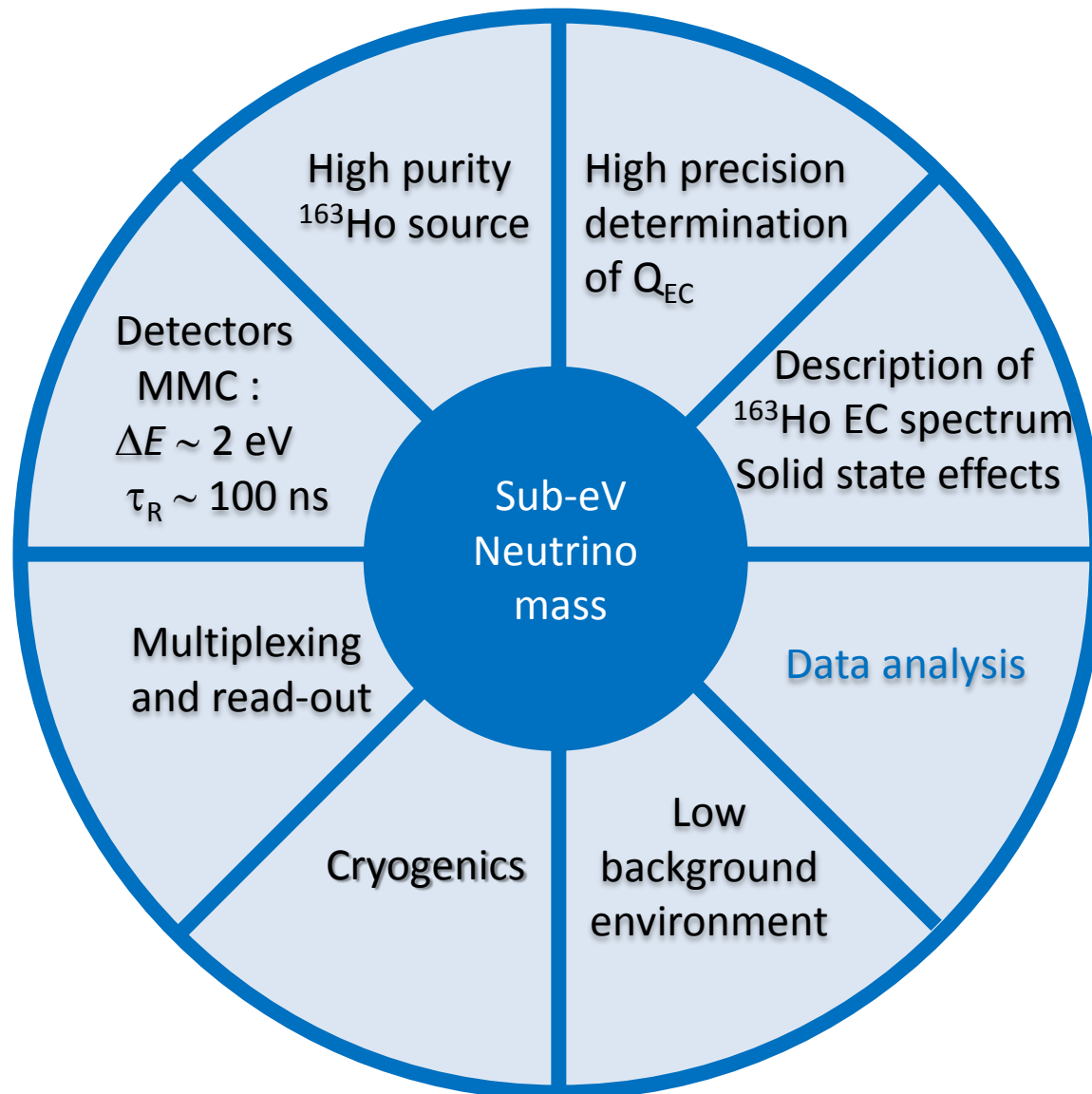
Core Level binding energy Shift (CLS):
calculated using the complete
screening approximation of DFT

Sensitivity to:

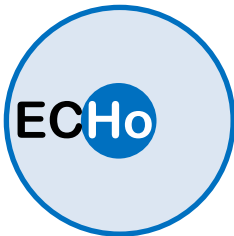
keV sterile neutrino

Cosmic neutrino background

ECHo experiment



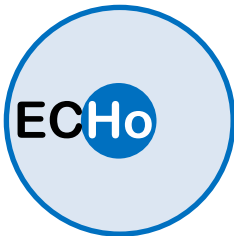
^{163}Ho experiments



- ◆ Started R&D in 2011
- ◆ Small scale experiment with ~100 pixels within the next three years
- ◆ Large scale experiment to reach sub-eV sensitivity to neutrino mass

<http://www.kip.uni-heidelberg.de/echo/>

^{163}Ho experiments



- ◆ Started R&D in 2011
- ◆ Small scale experiment with ~100 pixels within the next three years
- ◆ Large scale experiment to reach sub-eV sensitivity to neutrino mass

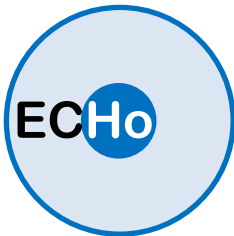
<http://www.kip.uni-heidelberg.de/echo/>



- ◆ Established in 2013 (ERC Advanced Grants for Prof. S. Ragazzi)
- ◆ Some R&D done already within the MARE experiment

<http://artico.mib.infn.it/nucriomib/general-infos/holmes-approved>

^{163}Ho experiments



- ◆ Started R&D in 2011
- ◆ Small scale experiment with ~100 pixels within the next three years
- ◆ Large scale experiment to reach sub-eV sensitivity to neutrino mass

<http://www.kip.uni-heidelberg.de/echo/>

HOLMES

- ◆ Established in 2013 (ERC Advanced Grants for Prof. S. Ragazzi)
- ◆ Some R&D done already within the MARE experiment

<http://artico.mib.infn.it/nucriomib/general-infos/holmes-approved>

OTHERS

- ◆ **LANL + NIST** (last two years)
 - investigation for source production
 - detector development for calorimetric measurements

<http://conference.ipac.caltech.edu/ltd-15> (Kunde, Schmidt, Croce, Fowler)

Conclusion

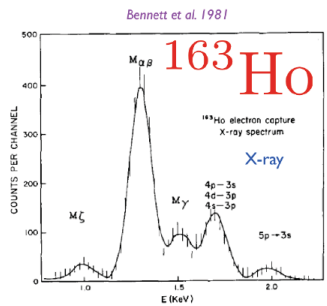


FIG. 5: IBEC spectrum in ^{163}Ho decay [22], showing prominent X-ray lines.

Some early measurements with a ^{163}Ho source [22, 23] were based on IBEC (Internal Bremsstrahlung in Electron Capture), the first-principle theory of which is fiendishly complex both above [24] and –more so– below [4] the energies coinciding with X-ray resonances. One example is shown in Fig. 5. Other measurements were calorimetric [25], see Fig. 6. The most stringent of the early mass limits, from [23] and [26] were, respectively:

$$\begin{aligned} m_\nu &< 225 \text{ eV at 95\% CL,} \\ m_\nu &< 490 \text{ eV at 68\% CL.} \end{aligned} \quad (8)$$

The recent progress may be illustrated by comparing Fig. 6 [25] with the preliminary results shown in Fig. 7, from the incipient experiment ECHo [27], which employs MMCs (Magnetic Metallic Calorimeters). The unlabeled peaks in Fig. 7 are due to ^{144}Pm , an impurity accompanying ^{163}Ho at the implantation stage at ISOLDE-CERN, an early test of source-preparation techniques.

One cannot resist the temptation of showing a scheme and a picture of the set of four MMCs in the ^{163}Ho detector prototype of ECHo [27]: Figs. 8 and 9. There is satisfaction associated with the possibility of measuring a tiny quantity –the neutrino mass– with nano-scale detectors. Even with the associated cryogenics and electronics, the apparatuses are still table-top.

V. THE THEORY OF EC IN ^{163}Ho

The EC process, all by itself, does not yield any information on the neutrino mass, or on anything else, for that matter. The mere information that “it happened” is

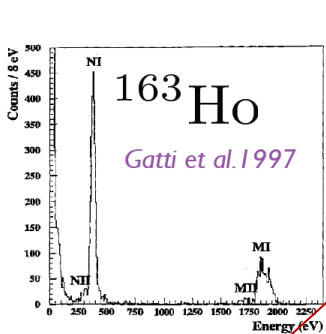


FIG. 6: Results of an early ^{163}Ho calorimetric spectrum [25].

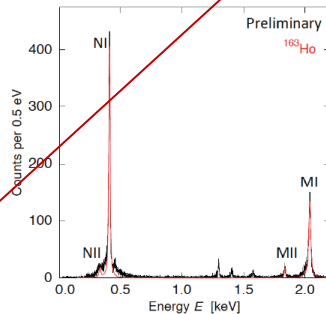


FIG. 7: Test results of ECHo [27] for the calorimetric spectrum of ^{163}Ho decay. The unlabeled impurities are ^{144}Pm . The continuous (red line) theory [5] is based on Eq. (9).

provided by the fact that the daughter atom, and sometimes its nucleus, are unstable. The hole in an atomic shell, for instance, results in observable X-rays, as the outer electrons cascade inwards, see Fig. 5.

The measured $Q = M(^{163}\text{Ho}) - M(^{163}\text{Dy})$ is so small that EC is only energetically allowed from ^{163}Ho orbitals with principal quantum number $n > 2$. The emission of X-rays from holes in such external shells is negligible compared to that of atomic de-excitations involving electron emission (in the classical parlance, the “fluorescence yields” are tiny). The electron-emitting transitions have

A. De Rujula

arXiv:1305.4857v1 [hep-ph] 21 May 2013

The recent progress may be illustrated by comparing Fig. 6 [25] with the preliminary results shown in Fig. 7, from the incipient experiment ECHo [27], which employs MMCs (Magnetic Metallic Calorimeters). The unlabeled peaks in Fig. 7 are due to ^{144}Pm , an impurity accompanying ^{163}Ho at the implantation stage at ISOLDE-CERN, an early test of source-preparation techniques.

One cannot resist the temptation of showing a scheme and a picture of the set of four MMCs in the ^{163}Ho detector prototype of ECHo [27]: Figs. 8 and 9. There is satisfaction associated with the possibility of measuring a tiny quantity –the neutrino mass– with nano-scale detectors. Even with the associated cryogenics and electronics, the apparatuses are still table-top.

Thank you!

[Department of Nuclear Physics, Comenius University, Bratislava, Slovakia](#)

Fedor Simkovic

[Department of Physics, Indian Institute of Technology Roorkee, India](#)

Moumita Maiti

[Institute for Nuclear Chemistry, Johannes Gutenberg University Mainz](#)

Christoph E. Düllmann, Klaus Eberhardt

[Institute of Nuclear Research of the Hungarian Academy of Sciences](#)

Zoltán Szűcs

[Institute for Theoretical and Experimental Physics Moscow, Russia](#)

Mikhail Krivoruchenko

[Institute for Theoretical Physics, University of Tübingen, Germany](#)

Amand Fäßler

[Kepler Center for Astro and Particle Physics, University of Tübingen](#)

Josef Jochum

[Kirchhoff-Institut for Physics, Heidelberg University, Germany](#)

Christian Enss, Andreas Fleischmann, Loredana Gastaldo,

Clemens Hassel, Sebastian Kempf,

Philipp Chung-On Ranitzsch, Mathias Wegner

[Max-Planck Institut for Nuclear Physics Heidelberg, Germany](#)

Klaus Blaum, Andreas Dörr, Sergey Eliseev

[Petersburg Nuclear Physics Institute, Russia](#)

Yuri Novikov

[Saha Institute of Nuclear Physics, Kolkata, India](#)

Susanta Lahiri

